INSTITUTE OF PLASMA PHYSICS

NAGOYA UNIVERSITY

Suppression of Beam-Excited Electron Waves by an Externally Applied RF Signal

Osamu Fukumasa and Ryohei Itatani

(Received - Oct. 21, 1980)

IPPJ-488 Nov. 1980

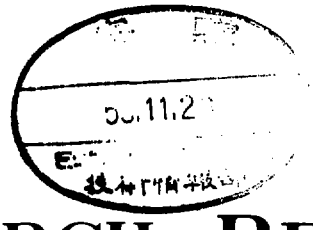

RESEARCH REPORT

NAGOYA, JAPAN

Suppression of Beam-Excited Electron Waves by an Externally Applied RF Signal

Osamu Fukumasa and Ryohei Itatani

(Received - Oct. 21, 1980)

IPPJ-488 Nov. 1980

Further communication about this report is to be sent to the Research Information Center, Institute of Plasma Physics, Nagoya University, Nagoya 464 Japan.

Department of Electronics, Kyoto University, Kyoto 606 Japan

ABSTRACT

Suppression of the beam-excited electron wave in a bounded system is investigated in connection with the beam distribution function. Wave suppression has two different processes depending on whether injected beams are reflected at the other end or not. In the absence of reflected beam electrons, deformation of the beam distribution function is observed in relation to the suppression of the electron wave. However, when beam electrons are reflected, the external wave suppresses the electron wave but distribution function shows no appreciable change.

These experimental results show that nonlinear behaviors of beam electrons, namely behaviors of reflected beams, are quite important for wave suppression. By using the method of partial simulation, interaction between two waves in the bounded system including nonlinear motions of beam electrons is studied numerically. Qualitative agreement between experimental and numerical results is obtained.

1. Introduction

Suppression of plasma waves such as electron waves and ion-acoustic waves, by appling an external ac signal, have been studied by many authors.[1-12] Among them, Keen and Fletcher reported[3] that an ion-acoustic instability excited in a plasma of arc discharge was suppressed by an external signal, and that this phenomena was phenomenologically explained by the Van der Pol equation with the external force term. Nakamura reported[4] that beam-excited longitudinal electron oscillations were suppressed by beam density modulation in an axially and transversely finite beam-plasma system. Similarly, he also explained these phenomena by assuming that the oscillations obeyed the Van der Pol equation with the external force term.

The above results do not, however, clearly delineate the physical processes involved in the wave suppression. In both cases,[3,4] the Van der Pol equation was derived by means of the fluid equations. The nonlinear terms, being essential to the Van der Pol equation, come from the source terms introduced supplementally in the continuity equation. In Ref.3, these source terms are interpretted as ionization etc. caused by large amplitude oscillations in the plasma. However, in collisionless plasma where the fluid theory is not applicable and no source term is present, it has been reported[13] recently that the Van der Pol equation is a phenomenological model for the ion-acoustic instability. Furthermore, it has been reported[14] that the oscillations in a bounded electron beam-plasma system with density modulation of the electron beam are governed by the Mathieu equation instead of the Van der Pol equation. Therefore, the theoretical basis for the Van der Pol equation can not be easily furnished within the framework of the hydrodynamic approximation.

Recently, there have been some experiments[8-12] where relationship between the wave suppression and the beam distribution function is studied in an electron beam-plasma system. These experimental results suggest that suppression mechanism must be considered including nonlinear behaviors of beam electrons.

The present paper gives the details of experimental measurements and a theoretical consideration for the suppression mechnism of beam-excited electron waves in a bounded system. Preliminary experiments have already been reported[8,9] in which deformation of the beam distribution function is observed in relation to the suppression of the electron waves. Further, this deformation depends strongly on whether the reflected beams are present or not.[10] In Section 2, the experimental arrangement and procedure are described. Section 3 contains the experimental results. The discussion is presented in Section 4. Finally, conclusions are presented in Section 5.

2. Experimental apparatus and methods

The experimental apparatus is shown schematically in Fig.1. In a cylindrical stainless steel chamber, with a length of 50 cm and a diameter of 10 cm, there are an electron gun, an energy analyzer and two axially movable probes. The base pressure of the chamber is about 2×10^{-6}Torr. The experiments are performed under continuous pumping and flowing of argon gas. The working pressure is about 10^{-4}- 10^{-3}Torr.

The electron gun continuously injects the electron beams with an acceleration voltage V_B up to an energy of several tens of electron volts, and a beam current I_B to 10 mA. A beam diameter is about 20 mm. The value of I_B can be controlled by changing a voltage of a grid V_G of the electron gun. The argon plasma is generated by the injected beam. An axial magnetic field of about 100 G is applied to confine radially the plasma and to obtain uniform density along the axial direction. Plasma parameters are as follows: electron density $n_e \cong 1 \times 10^8$ cm^{-3}, electron temperature T_e = 3-4 eV and the ratio of beam to plasma electron density $n_b/n_e \simeq (1\text{-}5) \times 10^{-2}$.

Oscillation signals are picked up by a coaxial probe with a diameter of 0.3 mm and a length of 2.5 mm, which is axially movable and is at floating potential, and are analyzed by means of a spectrum analyzer. This is also used as a Langmuir probe to measure plasma parameters.

In order to modulate the beam density, an external signal is applied to the grid G at various frequencies.

The velocity distribution function is measured by an energy analyzer or a plane probe with an area of 1×2 mm^2 perpendicular to

the magnetic field. After passing through the plasma column, the beam is collected in the analyzer. It is the conventional multigrid type, having two mesh grids and a collector plate. Plasma terminates at the front grid G_1. The second grid G_2 is used as the electron energy selector. The collector plate for the electron current I_c is kept at a positive potential of about 80 V. In order to obtain the electron velocity distribution function, it is necessary to take the first derivative of I_c with respect to the retarding voltage V_r.[15] This is carried out by a modulation method, where a small signal with voltage 100 mV_{p-p} and frequency 3.1 KHz is added to the dc retarding voltage. The ac component of I_c is proportional to the first derivative dI_c/dV_r. This measurement is carried out by the set-up shown in Fig.1. Distribution function along the plasma column is also obtained by the axially movable plane probe. Measurement method is the same as in the case of the analyzer described above.

In order to investigate the effects of reflected beams on wave suppression, experiments are performed under two different conditions. The one is with reflected beams, and the other without reflected beams. These two conditions are arranged by keeping the voltage of G_1 floating or earth potential. Figure 2 shows voltage-current characteristics of the plane probe. The plane is directed towards the analyzer so as to collect the reflected beams. It is clearly shown that reflected beam electrons are decreased to zero by increasing the voltage of G_1.

3. Experimental results

3.1 Beam-excited electron waves

Under certain conditions, electron waves are excited spontaneously in both cases, i.e. with and without reflected beam electrons. For unstable electron waves, discrete spectra are obtained, because injected beam and plasma produced by the beam are bounded by the anode A of the electron gun and G_1. The wavelength λ_n and the frequency f_n are roughly determined by the following relations:

$$\lambda_n = 2L/n \qquad \text{and} \qquad f_n = (n/2L)v_{pn}, \tag{1}$$

where a mode number n is an integer, L is the distance between A and G_1, and v_{pn} is the phase velocity of the wave.

Figure 3 shows a typical example of dependence of wave spectra and beam distribution functions on gas pressure in the absence of reflected beams. In this case, beam velocity v_b, i.e. V_B, and L are kept constant and argon pressure p is a parameter. When $p = 2.1 \times 10^{-4}$ Torr, the electron wave E_3 is excited spontaneously. The mode number n is three and its frequency f_3 is 44 MHz. With increasing p, the amplitude of E_3 becomes large and the width of the spectrum becomes broad, where $p = (2.3\text{-}2.9) \times 10^{-4}$Torr. Wave frequency also shifts to higher side. With increasing p further, the wave mode is changed to next higher mode, where $p = (3.6\text{-}4.6) \times 10^{-4}$Torr. In relation to these changes of wave spectra, beam distribution functions are also deformed. Not collisional effects, i.e. gas pressure, but wave intensity and the shape of wave spectrum are effective to deform the beam distribution.

When $p = 3.8 \times 10^{-4}$Torr and $V_B = 37$ V, the wave E_3 with frequency 53 MHz is excited and has the same spectrum as that in the case, where $p = (2.1\text{-}2.3) \times 10^{-4}$Torr. Then the resulting beam distribution has the same pattern as that in the case, where $p = (2.1\text{-}2.3) \times 10^{-4}$Torr.

Figure 4 shows some features of beam distribution functions and wave spectra in the presence of reflected beams. In this case, V_B, L and p are kept constant. The voltage of the grid of the gun V_G is a parameter. There is a best condition where a certain mode has its maximum amplitude. With incresing V_G, the amplitude of E_4 becomes large and E_4 has the maximum amplitude when $V_G = -32$ V. With increasing V_G further, the amplitude of E_4 becomes small and the next higher mode E_5 appears. A mode-jump is also observed by changing p as shown in Fig.3. In the course of the change of wave spectrum, there is no appreciable change in the width of the wave spectrum. The width at half-maximum is about 0.5 MHz throughout the present experiment. Beam distribution is deformed little by little as the wave amplitude becomes large and multimode are excited.

In order to study the suppression mechanism in relation to the beam distribution, it is necessary to deal with the case where a single mode with a narrow frequency spectrum is excited. Because, in this case, we can consider the interaction between only two waves, i.e. the electron wave and the externally excited wave.

3.2 Suppression of electron waves in the absence of reflected beams

Before doing experiments of wave suppression, we show the dependence of wave frequency on system length L. Typical row data of wave spectrum and the relationship between the wave frequency and the reciprocal of

L are shown in Fig.5. With decreasing L, wave frequency shifts to the higher side and a mode jump occurs at about L = 12.5 cm. This frequency shift is proportional to the reciprocal of L.

If we set L = 11 cm, only the wave E_2 is excited spontaneously. As is shown later, wave suppression is strongly dependent on modulation frequency f_m. In the case shown in Fig.5(b), effects of beam modulation is very strong when f_m is close to the frequency of E_2 and in the shaded region. The shaded region is the frequency of E_3 neighboring with E_2 appearing spontaneously.

When the beam density is modulated by applying an external signal with f_m to G, the excited wave E_m with the same frequency is observed. The amplitude of E_m becomes large as the modulation voltage V_m of the signal is increased. The amplitude of the electron wave can be controlled by the excited wave.

Two examples of wave suppression are shown in Fig.6. In the case of (a), the electron wave E_1 with frequency 14.8 MHz is excited spontaneously and f_m is chosen to be the vicinity of f_1. With increasing V_m, the amplitude of E_m increases and that of E_1 decreases. When $V_m = 0.8\ V_{p-p}$, E_1 is suppressed and only E_m is observed.

As is mensioned above, when f_m is chosen to be close to the frequency of the neighboring mode which is not excited spontaneously, similar phenomena is occured. Figure 6(b) shows this case. The electron wave E_2 with frequency 34 MHz is excited spontaneously. f_m is set to 49.5 MHz which is close to that of the electron wave E_3 not excited spontaneously. When $V_m = 1\ V_{p-p}$, E_2 is suppressed.

The critical modulation voltage V_c, above which the electron wave is suppressed by the beam modulation, is dependent on f_m.

Relationship between V_c and f_m is shown in Fig.7(a), where the wave E_4 with frequency 51 MHz is excited. The value of V_c is nearly proportional to the frequency difference between f_m and the frequency of E_4, i.e. $|f_m - f_4|$. The amplitude of the excited wave ϕ_c, which is observed when $V_m = V_c$, is plotted as a function of f_m. For reference, the amplitude of E_4 without modulation is also poltted by the dotted circle. These wave amplitudes are measured by using the coaxial probe which is set to the fixed point. It is said that ϕ_c is larger than the amplitude of E_4, and that the relationship between ϕ_c and f_m is not so clear as the relationship between V_c and f_m.

In order to understand the axial dependence of the excited wave, wave spectrum is measured by moving the coaxial probe along the plasma column. Three wave patterns of the excited wave are shown in Fig.7(b), where three values of V_m correspond to V_c at each f_m respectively. It is found that throughout the plasma column every amplitude of the excited wave is larger than the amplitude of E_4.

The change of the beam distribution function is observed in relation to the wave suppression. Figure 8 shows the distribution function F(V), measured by the analyzer, corresponding to the case shown in Fig.7. The bottom trace of the dashed line is F(V) without beam modulation. Comparing this with the deformed distributions, it is found that additional broadening or the degree of the deformation of F(V) becomes remarkable as f_m approaches to f_4. However, at the same time, the value of V_c becomes minimum.

These features shown in Figs.7 and 8 are also obtained in the case where f_m is chosen to be nearly equal to the frequency of the neighboring mode. For example, Fig.9 shows the relationship between

f_m and V_c, and f_m and ϕ_c.

In order to clear the relation between the wave suppression and the deformation of F(V), wave patterns and beam distributions are also measured simultaneously. A value of V_m is a parameter. One example of these measurements is shown in Figs.10 and 11. In Fig.10, wave patterns of the electron wave E_2 and those of the excited wave E_m are shown for various modulation voltages. With increasing V_m, the amplitude of E_m becomes large and that of E_2 becomes small. It is also found that no remarkable shift of wave pattern occurs axially, namely amplitudes of waves are varied by beam modulation without changing positions of their nodes and antinodes. Corresponding deformation of F(V) is shown in Fig.11. The degree of the deformation becomes large as V_m is increased. It is important that a remarkable change of F(V) is observed already before E_2 is suppressed. When $V_m = 2.1\ V_{p-p}$, E_2 is almost suppressed. At the same time, F(V) changes to be more broader and the shape of F(V) may be a double-humped distribution about the phase velocity of E_m.

It is not fruitful to discuss the fine structure of F(V) further. Because the final shape of F(V) depends strongly on the shape of F(V) without modulation although the change of F(V) is caused by the presence of E_m. As is shown in Fig.3, the shape of F(V) without modulation depends on some plasma conditions, i.e. V_B, p, L etc., which determine the character of the electron wave excited spontaneously. We can only say that deformation of F(V) occurs and F(V) becomes broader in relation to the suppression of the electron wave.

So far, only the deformation of F(V) which are measured at the end of plasma column is reported. Spatial dependence of the change

of F(V) is also measured. Figure 12(a) shows trace of F(V) at various positions. As the amplitude of E_2 excited spontaneously is small in this case, suppression of E_2 occurs with a weak modulation, i.e. $V_c = 0.5\ V_{p-p}$. The energy at the peak of F(V), obtained from Fig.12(a), and the amplitude of E_m are plotted versus axial position in Fig.12(b). On the change of F(V) along the plasma column, there is a following tendency. The width of F(V) becomes broader at a posterior region. F(V) is velocity-modulated corresponding to the wave pattern of E_m. However, this type of deformation may be measured clearly when suppression occurs with a small value of V_c and the mode number of the wave is also small. Otherwise, broadening process becomes remarkable and the fine structure of velocity modulation is masked.

Figure 13 is another example concerning the spatial dependence of the change of F(V). It shows deformation of F(V) at three different points, relating to the suppression of the electron wave E_3. When $V_m = 1.1\ V_{p-p}$, E_3 is almost suppressed. It is also found that the degree of the change of F(V) due to the presence of E_m becomes remarkable as the distance from A becomes long.

Finally, we note that throughout these experiments, distribution function of the background plasma shows no appreciable change.

3.3 Suppression of electron waves in the presence of reflected beams

When the voltage of G_1 is kept at floating potential which is nearly equal to the beam acceleration voltage V_B, beam electrons passing through the plasma column are reflected at G_1 and feedback effects of reflected beams are present. Although suppression phenomena in the same system was studied by several authors,[4,7] relationship between wave suppression

and beam distribution was not discussed in detail. Recently, Amemiya reported[12] the results of measurements of F(V) in the counter stream beam-plasma system, where a remarkable change of F(V) was not observed in relation to wave suppression. We also study the wave suppression in the presence of reflected beams so as to compair the results with those in the absence of reflected beams. Experimental results are shown briefly.

Typical examples of wave suppression at various modulation frequency are shown in Fig.14. In the present experiment, f_m is chosen so that the frequency difference between f_m and f_4 is smaller than 1 MHz. Then, wave suppression occurs with a rather weak modulation. With increasing V_m, the amplitude of the electron wave E_4 decreases as that of the excited wave becomes large. Values of V_c decreases as f_m approaches to f_4 = 38.5 MHz. As a whole, these characteristics are the same as those obtained in the absence of reflected beams.

There are, however, some different features. The resulting amplitude of the excited wave is nearly equal to the amplitude of E_4, manely wave suppression may occur under the constant wave energy. It is also found that in the course of wave suppression a side band wave[16] with frequency $2f_4-f_m$ or $2f_m-f_4$ appears more remarkably than one does in the absence of reflected beams.

Relationship between V_c and f_m is shown in Fig.15. The resulting amplitude of the excited wave is also plotted. The frequency width Δf at half-maximum of frequency spectrum of E_4 is about 0.5 MHz. When the frequency difference $|f_4 - f_m|$ is within Δf, the value of V_c is relatively small. The amplitude of the excited wave corresponding to V_c is also comparable to that of E_4, namely total wave energy has

constant value. As $|f_4 - f_m|$ exceeds Δf, however, the value of V_c increases sharply. Then, the resulting amplitude of E_m becomes larger than that of E_4 and the change of F(V) is observed.

In relation to the wave suppression, measurement of F(V) has been done and the results are shown in Fig.16. Experimental conditions are nearly the same as those in Fig.15. Parameters are f_m and V_c. The bottom trace is the distribution function without modulation. Obviously, wave suppression occurs without appreciable change in F(V), when f_m is nearly equal to f_4. However, as $|f_4 - f_m|$ exceeds Δf, values of V_c becomes large abruptly. Then, wave suppression is accompanied with deformation of F(V).

4. Discussion

Observed electron waves are excited by the coupling of the slow space charge wave of the beam with the longitudinal electron wave of the plasma. When a beam-plasma system is bounded in both the longitudinal and transverse directions, the wave frequency ω can either be equal to the electron plasma frequency ω_{pe} or considerably lower than ω_{pe} depending on the relation between the wavelength λ and the transverse dimension of the beam radius a.[17] In the present system, dispersion relation can be written as follows:

$$\left\{ \frac{\omega_{pe}^2}{\omega^2} + \frac{\omega_b^2}{(\omega - kv_b)^2} \right\} F^2 = 1 , \qquad (2)$$

$$F^2 = \frac{(ka)^2}{2} \ln(1/ka) \quad , \quad (ka \ll 1) \qquad (3)$$

where ω_b is the electron plasma frequency of the beam, v_b is the drift velocity of the beam, and k is the wave number. We assume that the motion of particles across the beam can be neglected. This is equivalent to the assumption that a rather strong magnetic field acts along the beam(electron cyclotron frequency $\omega_{ce} \gg \omega$). The ration $\omega/\omega_{ce} \simeq 1/6$. It is also assumed that both the beam and plasma are cold and that the radius of plasma is equal to that of beam. Then, the frequency of the excited oscillation is not ω_{pe} but $F\omega_{pe}$ in resonance. From electron density measured by the Langmuir probe, the ratio of the observed oscillation frequency to the electron plasma frequency are determined. For example, in Fig.6(b) the electron wave E_2 with frequency f_2 = 34 MHz is excited and the measured ratio f_2/f_{pe} = 0.38, where $n_e \simeq 1 \times 10^8$ cm^{-3}. The evaluated ratio $f/f_{pe} = F$ from eq.(3) is about equal to 0.3, where

$a \simeq 1$ cm and $\lambda \cong 10$ cm.

In the previous chapter, we have presented the experimental results on suppression of beam-excited electron waves due to beam density modulation. They are summarized as follows: In the absence of reflected beams, deformation of the beam distribution function is observed in relation to suppression of the electron wave. In the presence of reflected beams, however, the electron wave can be replaced by the excited wave under the constant distribution function of beam electrons.

Besides, the manner of interaction between the electron wave and the excited wave depends strongly on whether or not reflected beams are present. This is clearly shown in Figs. 17 and 18. It looks that with increasing V_m, the excited wave increases and the electron wave decreases independently each other when reflected beams are absent(see Fig.17). However, when reflected beams are present, interaction between two waves is strong. The most striking feature is that the rapid change in the ratio of wave intensities occurs when the excited wave grows up to a certain level with increasing V_m. This rapid change may be a consequence of the so-called mode competition.[18]

Usually, experiments on wave suppression have been explained by using the phenomenological model of the Van der Pol equation with external force term.[3,4] Experimental results in the presence of reflected beams may be described by this model. But, this model can not describe the beam dynamics and the results in the absence of reflected beams must be considered by using another model. Because, the deformation process of the beam distribution function is essentially based on the nonlinear beam-plasma interaction. Besides, experimental results suggest that feedback effects of reflected beams are quite important for wave suppression.

Therefore, by means of not the Van der Pol model but a particle picture, we discuss our experimental results in both cases systematically. Throughout the present experiments, we control the plasma paremeters so that single mode electron wave with sharp frequency spectrum is excited spontaneously. The excited wave due to beam modulation also has a sharp spectrum. In the course of wave suppression, it is also found that the electron wave and the excited wave predominate the nonlinear beam-plasma interaction. The higher harmonics of these two waves or the sideband mode are much smaller than the electron or the excited wave. Therefore, we shall consider that only two waves, namely the electron wave and the excited wave, determine the nonlinear behaviors of beam electrons in the bounded system.

In order to investigate the experimental results including nonlinear beam dynamics in the presence of two waves, the method of partial numerical simulation is used.[19,20] This technique assumes that the plasma response remains linear and can be described through its dielectric properties, while the beam trajectories are calculated exactly. In the present analysis, the plasma is described through the linearized fluid equations.

The present model simulates a one-dimensional fixed plasma with the system length L, where beam electrons are injected continuously at the left end of the system, namely $x = 0$. According to experimental conditions, two different boundary conditions at the right end of the system, namely $x = L$, are imposed on beam particles. The one is the case of absorption. Beam particles which drift out the right end of the system are removed without contributing to the electric field. The other is the case of reflection. Beam particles which drift out the

right end are reentered into the system with conditions, i.e. position $x_j = 2L - x_j$ and velocity $v_j = -v_j$ of the j-th beam particle. These reflected beams which drift out the left end of the system are removed.

Periodic boundary conditions are imposed on waves. Then, we assume the following form of the electron wave including the effects of backward wave,

$$E(x,t) = E_k(t)\cdot e^{-i\omega_k t}(e^{ikx} + R\cdot e^{-ikx}) + C.C. \qquad (4)$$

where $E_k(t)$ is slowly varying function, $k = 2\pi m/L$, m is an integer, ω_k is the characteristic frequency of the mode k, and R is the reflection coefficient. Effect of beam modulation is introduced into Poisson's equation by an external oscillating charge density described as follows:

$$\rho_m = \rho_0 \cos(\omega_m t)\cdot [\ \delta(x-X_0+\frac{\delta}{2}) - \delta(x-X_0-\frac{\delta}{2})\ ] \qquad (5)$$

where ρ_0 is external charge density, ω_m is a modulation frequency, X_0 is the position of near the left end, and a pair grid with spacing δ is located at X_0. Here, we consider the case that ω_m is nearly equal to ω_k, i.e. $\omega_m = \omega_k + \delta\omega$ and $\delta\omega \ll \omega_k, \omega_m$. We also assume the following form of the external wave

$$F(x,t) = F_k(t)\cdot e^{-i\omega_m t}(e^{ikx} + R\cdot e^{-ikx}) + C.C. \ , \qquad (6)$$

where $F_k(t)$ is slowly varying function. Time evolutions of $E_k(t)$, $F_k(t)$, and the position $X_j(t)$ and the velocity $V_j(t)$ of the j-th beam particle are solved numerically. The orbits of the beams are solved in the single wave approximation before the application of beam modulation. After this,

they are solved in the two wave approximation. The set of equations to be solved are as follows:

$$\frac{d^2E_\kappa}{dt^2} - i2\omega_\kappa \frac{dE_\kappa}{dt} = \frac{4\pi e n_b}{N}\sum_j \left[\frac{d}{dt}\left(v_j e^{-i\kappa x_j}\right)\right]\cdot e^{i\omega_\kappa t} - \frac{4\pi\omega_m^2}{\kappa L}\rho_0 \sin\frac{\kappa\delta}{2}\left[e^{i(\omega_m+\omega_\kappa)t} + e^{-i(\omega_m-\omega_\kappa)t}\right]e^{-i\kappa x_0}, \tag{7}$$

$$\frac{d^2F_\kappa}{dt^2} - i2\omega_m \frac{dF_\kappa}{dt} - (\omega_m^2 - \omega_\kappa^2)F_\kappa = \frac{4\pi e n_b}{N}\sum_j \left[\frac{d}{dt}\left(v_j e^{-i\kappa x_j}\right)\right]\cdot e^{i\omega_m t} - \frac{4\pi\omega_m^2}{\kappa L}\rho_0 \sin\frac{\kappa\delta}{2}\left(e^{i2\omega_m t} + 1\right)e^{-i\kappa x_0}, \tag{8}$$

and

$$\frac{d^2x_j}{dt^2} = -\frac{e}{m}E_\kappa e^{-i\omega_\kappa t}\left(e^{i\kappa x_j} + R\cdot e^{-i\kappa x_j}\right) - \frac{e}{m}F_\kappa e^{-i\omega_m t}\left(e^{i\kappa x_j} + R\cdot e^{-i\kappa x_j}\right) + C.C. \tag{9}$$

where n_b is the beam density and N is the initial total number of beam particles in the system.

Before presenting the numerical results of the simulation, we consider further the terms of the right hand side in eqs.(7) and (8), which represent the effects of beam electrons. By taking into account the perturbation of the orbit of a beam particle, the terms can be represented as a function of $E_k(t)$ and $F_k(t)$. Then, a nonlinear rate equations for $E_k(t)$ and $F_k(t)$ are obtained and the role of reflected beam electrons is also clearified. After some algebra (described briefly in Appendix), we find the following form of the rate equations

$$\frac{dE_\kappa}{dt} = \alpha_1 E_\kappa - \beta_1 E_\kappa^3 - \theta_{12} F_\kappa^2 E_\kappa , \tag{10}$$

$$\frac{dF_\kappa}{dt} = \alpha_2 F_\kappa - \beta_2 F_\kappa^3 - \theta_{21} E_\kappa^2 F_\kappa . \tag{11}$$

In the two wave system described above,[18,21] the mode competition arises from the θ terms. When the reflected beams are present, the θ terms brcomes large due to the effects of interaction between the reflected beams and the backward wave. Consequently, the mode coupling may become strong. It is reasonable that the rapid change in the ratio of wave intensities occurs in the system where reflected beams are present(see Figs.17 and 18).

Similar results described above have been also derived by some authors. Walsh and Hagelin[22] obtained a kind of Van der Pol equation by expanding the beam-plasma dispersion relation around the most unstable root and the perturbed beam electron orbit. Janssen and Rasmussen[23] showed that the dynamical equation for the bump-on-tail instability was given by the well-known nonlinear Landau equation. In both cases, wave-particle interaction may be considered as a candidate for the origin of nonlinear terms essential to the wave suppression.

Now, we are in the position to discuss the results of simulation. For performing numerical calculation, dimensionless variables are introduced as follows: The temporal coordinate $\tau = s\omega_k t$, the normalized electric field $E(\tau) = ekE(t)/(ms^2\omega_k^2)$, and the temporal scaling factor $s = (n_b/2n_e)^{1/3}$. Mean beam velocity $V(\tau)$ and the beam velocity spread ΔV_b are also obtained as a function of τ. These values are defined as follows:

$$V(\tau) = \sum_{j=1}^{M} V_j(\tau)/M \qquad \text{and} \qquad (\Delta V_b)^2 = \sum_{j=1}^{M} (V_j(\tau) - V(\tau))^2/M, \qquad (12)$$

where M is the total number of beam particles at each time step in the system.

Numerical calculations are performed under various plasma conditions. Here, typical examples are shown and discussed compairing with the experimental results. The result of the first case, where injected beams are absorped at the right end, x = L, is shown in Fig.19. The unstable electron wave grows exponentially and saturates its amplitude at τ = 10. After this point, the wave has constant amplitude in the case of no modulation(shown by dashed line). Corresponding to the evolution of the wave amplitude, beam spread also becomes large up to the saturation point of the wave amplitude and has nearly the constant spread in the later region. Beam modulation is introduced at τ = 14. Then, with the growth of the external wave, the electron wave decreases in amplitude up to τ = 20.3. After this point, energy exchange between the electron wave and the external wave occurs. The additional broadening of the beam distribtuion also occurs with the introduction of beam modulation. The time evolution of the beam spread corresponds to that of the total wave energy not shown in Fig.19.

The result of the second case, where injected beams are reflected at the right end of the system, x = L, is shown in Fig.20. In the initial stage, beam electrons with velocity V_b and with $-V_b$ are distributed uniformly throughout the system. The electron wave grows up and saturates its amplitude at τ = 14. Corresponding to the wave growth, the spread of the forward beam becomes large till τ = 14. After this point, beam distribution keeps nearly the constant value of the spread as the wave has nearly the constant amplitude. Beam modulation is introduced at τ = 18 when the wave amplitude is saturated already. The electron wave decreases in amplitude up to τ = 28, while the external wave grows larger. After this point, energy exchange between two waves also

occurs as that does in the absence of reflected beams. However, there is some different features in this case. In spite of the excitation of the external wave, total wave energy has nearly the constant value. After the time τ = 25, it becomes larger gradually. Corresponding to the evolution of total wave energy, the spread of beam distribution has nearly the constant value. Namely, up to the time τ = 28, the change of wave intensities occurs under nearly the constant value of total wave energy and the additional broadening of the beam distribution does not occur appreciably.

In both cases, up to the first minimum of the electron wave, the numerical results on the suppression process of the electron wave have the same features as the experimental ones do, respectively.

Experimentally, measurements of wave amplitudes and beam distribution function are carried out under the steady-state conditions, where the electron wave and the external wave with constant amplitudes, respectively, are present corresponding to various strength of beam modulation. This state is not observed in the simulation, because amplitude oscillations due to the energy exchange between two waves occur after the first minimum of the electron wave. This may be due to the lack of support for the perfect phase lock in the code. In a real experiment, however, a certain state is determined by the nonlinear behavior of the injected and reflected beams in the presence of the wave fields. When the suppression of the electron wave occurs, the beam electrons are locked to the bounded state by the excited wave. However, in the present simplified model, boundary conditions of the beam and those of the wave including the reflection coefficient are not determined self-consistently, but are assumed to have a certain condition independently each other.

Now, we estimate the reflection coefficient R in the present experiments. The value of R is obtained from the voltage standing wave ratio R_{vswr} of the wave pattern. For this purpose, amplitudes at the anti-node and the node nearest to the grid G_1 are used because the effects of reflection appear most remarkably. When the beam electrons are absorped at G_1, R_{vswr} is from 2.2 to 3.1. Then, R is from 0.37 to 0.51. When the beam electrons are reflected at G_1, R_{vswr} is from 5.8 to 7. Then, R is from 0.7 to 0.75. Above numerical results are obtained when R = 1. Similar results are also obtained when R = 0.5. Difference between the numerical results of two cases, i.e. with or without reflected beams, is caused mainly by whether the feedback effects of reflected beams are present or not.

In many situations, collisions between plasma electrons and neutral atoms or ions play an important role in the development of a beam-plasma instability. They can become the deciding factor in limiting the temporal or spatial growth and determining its magnitude. In cases where the beam has a finite velocity spread, collisions drastically reduce the growth rate, and the delicate interplay of collision frequency and velocity spread of the beam can lead to a quenching of the instability.[24)]

In the present system, electron-neutral collision is predominant. We estimate the collision frequency ν_{e-n} under the following conditions: $\varkappa T_e \simeq 3$ eV, $p = 2 \times 10^{-4}$ Torr and $n_e \simeq 1 \times 10^8$ cm^{-3}. Thermal velocity of the plasma electron v_{te} is about 1.03×10^8 cm/sec. Mean free path of plasma electron l_{mfs} is about 250 cm. Then, $\nu_{e-n} = v_{te}/l_{mfs} = 0.43$ MHz and $2\pi\nu_{e-n}/\omega_p = 4.6 \times 10^{-3}$. So , this system is considered as the collisionless system and the collisional effects is not so important as ones in other systems.[12,24)] However, the present authors have shown

that in the semi-infinite space, nonlinear interaction between a small cold beam and a plasma can be changed drastically by introducing weak collisions of the order of $\nu/\omega_p \sim 10^{-3}$ within the background plasma.[25] So, in the present model, numerical calculation with collisional effects has also been performed, where $\nu/\omega_p = 10^{-2}$. But, in the bounded system described above, anomalous effects due to weak collisions do not occur except that the saturation amplitude decreases slightly at a lower level.

5. Conclusion

We have considered the suppression of beam-excited electron waves experimentally in a bounded beam-plasma system. Experimental conditions have been controlled carefully so that a single mode of the electron wave with sharp frequency spectrum is excited spontaneously. Two types of wave suppression processes are observed. They depend on whether feedback effects of reflected beams are present or not.

In the absence of reflected beam electrons, deformation of the beam distribution function is observed in relation to the suppression of the electron wave. When beam electrons are reflected, however, the excited wave suppresses the electron wave but beam distribution function shows no appreciable change. In these two cases, distribution function of background plasma electrons shows no appreciable change. It is also found experimentally that only the electron and the excited waves predominate in the process of the wave suppression.

By using the method of partial simulation, interactions between two waves including nonlinear motions of beam electrons is studied. Salient features of the experimental results in two cases, namely with or without reflected beams, are corroborated by the numerical solutions.

These experimental and numerical results show that nonlinear behaviors of beam electrons are quite important for deciding the suppression process of the wave. Present consideration may be applicable to the suppression of the ion-acoustic wave which has the same dispersion relation as the beam-excited electron wave.

Acknowledgement

The authors wish to thank Drs. H. Abe, Kyoto University and H. Naitou, Institute of Plasma Physics at Nagoya University for their discussions on the simulation model. It is also a pleasure to thank Dr. J. J. Rasmussen, Risφ National Laboratory in Denmark, for his discussion concerning the suppression mechanism.

This work was partially supported by the Grant-in-Aids for Scientfic Research of the Ministry of Education, Science and Culture.

A part of this work was also supported by the Collaborating Research Program at the Institute of Plasma Physics, Nagoya University.

Numerical calculations were perfomed at the Data Processing Center of Kyoto University and at the Institute of Plasma Physics, Nagoya University.

Appendix

In this appendix, we show the outline of derivation of eqs.(10) and (11). In order to obtain the rate equations, it is sufficient to examine the following approximate equations which are derived from eqs. (7)-(9),

$$\frac{dE_\kappa}{dt} = -\frac{2\pi e n_b}{\omega_\kappa N}\sum_j \frac{dV_j}{dt}\cdot\sin(\omega_\kappa t-\kappa x_j)+\frac{\pi e n_b \kappa}{\omega_\kappa N}\sum_j V_j^2\cos(\omega_\kappa t-\kappa x_j)\,, \tag{A.1}$$

$$\frac{dF_\kappa}{dt} = -\frac{2\pi e n_b}{\omega_m N}\sum_j \frac{dV_j}{dt}\cdot\sin(\omega_m t-\kappa x_j)+\frac{\pi e n_b \kappa}{\omega_m N}\sum_j V_j^2\cos(\omega_m t-\kappa x_j)\,, \tag{A.2}$$

and

$$\frac{d^2x_j}{dt^2} = \frac{dV_j}{dt} = -\frac{2e}{m}\Big[E_\kappa\cdot\cos(\omega_\kappa t-\kappa x_j)+R\cdot E_\kappa\cos(\omega_\kappa t+\kappa x_j) + F_\kappa\cdot\cos(\omega_m t-\kappa x_j)+R\cdot F_\kappa\cos(\omega_m t+\kappa x_j)\Big]\,. \tag{A.3}$$

The terms $E_k(t)$ and $F_k(t)$ vary slowly compared to the high frequency ω_k and ω_m, we may neglect the second order derivative. For example, assuming that $E_k = E_k(0)\cdot e^{\gamma t}$ where γ is the linear growth rate, the ratio $2\omega_k(dE_k/dt)/|d^2E_k/dt^2| = 2\omega_k/\gamma \simeq 2(2n_e/n_b)^{1/3}$. As $n_b/n_e \simeq 10^{-2}$ in the present experiments, the above ratio is about 12. The terms due to beam modulation are also neglected, because they are the external source terms and not important for the derivation of the nonlinear rate equations. Lastly, we assume that E_k and F_k are real quantities. Strictly speaking, they are complex quantities because system has a nonlinear phase shift. But, in order to discuss and describe the suppression of instability by an external wave, only the amplitude variation is of importance.

Next, we consider the perturbation of the orbit of the j-th beam particle. Let the forward beam, i.e. the injected beam

$$X_j(t) = X_j(0) + V_0 t + \delta X_j \tag{A.4}$$

then,

$$\frac{d^2 x_j}{dt^2} = \delta \ddot{x}_j = -\frac{2e}{m} E_0 \left[e^{\gamma t} \cos\{\kappa \delta x_j + \eta_0 t + \kappa x_j(0)\} + R \cdot e^{\gamma t} \cos\{\kappa \delta x_j + \eta_1 t + \kappa x_j(0)\} \right]$$
$$-\frac{2e}{m} F_0 \left[e^{\gamma' t} \cos\{\kappa \delta x_j + \eta_0' t + \kappa x_j(0)\} + R \cdot e^{\gamma' t} \cos\{\kappa \delta x_j + \eta_1' t + \kappa x_j(0)\} \right] \tag{A.5}$$

Let the backward beam, i.e. the reflected beam,

$$X_j(t) = X_j(0) - V_0 t + \delta X_j \tag{A.6}$$

then,

$$\delta \ddot{x}_j = -\frac{2e}{m} E_0 \left[e^{\gamma t} \cos\{\eta_1 t - \kappa x_j(0) - \kappa \delta x_j\} + R \cdot e^{\gamma t} \cos\{\eta_0 t - \kappa x_j(0) - \kappa \delta x_j\} \right]$$
$$-\frac{2e}{m} F_0 \left[e^{\gamma' t} \cos\{\eta_1' t - \kappa x_j(0) - \kappa \delta x_j\} + R \cdot e^{\gamma' t} \cos\{\eta_0' t - \kappa x_j(0) - \kappa \delta x_j\} \right] \tag{A.7}$$

where $\eta_0 = kV_0 - \omega_k$, $\eta_1 = kV_0 + \omega_k = \eta_0 + 2\omega_k$, $\eta_0' = kV_0 - \omega_m = \eta_0 - \delta\omega$, $\eta_1' = kV_0 + \omega_m = \eta_0 + 2\omega_k + \delta\omega$, and γ and γ' are the linear growth rates of the electron and the excited waves, respectively. A value of $\delta\omega$ is the frequency difference between ω_k and ω_m. Linearizing the eqs.(A.5) and (A.7), we can obtain the slow time varying part of the orbit perturbation as follows:

The forward beam

$$\delta V_j = -\frac{2e}{m} \cdot \frac{E_\kappa(t)}{\alpha_0^2} \left[(\gamma \cos\eta_0 t + \eta_0 \sin\eta_0 t - \gamma e^{-\gamma t}) \cos\kappa x_j(0) \right.$$
$$\left. - (\gamma \sin\eta_0 t - \eta_0 \cos\eta_0 t + \eta_0 e^{-\gamma t}) \sin\kappa x_j(0) \right]$$
$$-\frac{2e}{m} \cdot \frac{F_\kappa(t)}{\alpha_1^2} \left[(\gamma' \cos\eta_0' t + \eta_0' \sin\eta_0' t - \gamma' e^{-\gamma' t}) \cos\kappa x_j(0) \right.$$
$$\left. - (\gamma' \sin\eta_0' t - \eta_0' \cos\eta_0' t + \eta_0' e^{-\gamma' t}) \sin\kappa x_j(0) \right] \tag{A.8}$$

$$\delta x_j = -\frac{2e}{m}\cdot\frac{E_K(t)}{a_0^4}\Big[\big(b_0^2\cos\eta_0 t + 2\gamma\eta_0\sin\eta_0 t - b_0^2 e^{-\gamma t} - \gamma a_0^2 t e^{-\gamma t}\big)\cos Kx_j(0) - \big(b_0^2\sin\eta_0 t - 2\gamma\eta_0\cos\eta_0 t + 2\gamma\eta_0 e^{-\gamma t} + \eta_0 a_0^2 t e^{-\gamma t}\big)\sin Kx_j(0)\Big]$$

$$-\frac{2e}{m}\cdot\frac{F_K(t)}{a_1^4}\Big[\big(b_1^2\cos\eta_0' t + 2\gamma'\eta_0'\sin\eta_0' t - b_1^2 e^{-\gamma' t} - \gamma' a_1^2 t e^{-\gamma' t}\big)\cos Kx_j(0) - \big(b_1^2\sin\eta_0' t - 2\gamma'\eta_0'\cos\eta_0' t + 2\gamma'\eta_0' e^{-\gamma' t} + \eta_0' a_1^2 t e^{-\gamma' t}\big)\sin Kx_j(0)\Big] \qquad (A.9)$$

the backward beam

$$\delta v_j = -\frac{2e}{m}\cdot\frac{R E_K(t)}{a_0^2}\Big[\big(\gamma\cos\eta_0 t + \eta_0\sin\eta_0 t - \gamma e^{-\gamma t}\big)\cos Kx_j(0) + \big(\gamma\sin\eta_0 t - \eta_0\cos\eta_0 t + \eta_0 e^{-\gamma t}\big)\sin Kx_j(0)\Big]$$

$$-\frac{2e}{m}\cdot\frac{R F_K(t)}{a_1^2}\Big[\big(\gamma'\cos\eta_0' t + \eta_0'\sin\eta_0' t - \gamma' e^{-\gamma' t}\big)\cos Kx_j(0) + \big(\gamma'\sin\eta_0' t - \eta_0'\cos\eta_0' t + \eta_0' e^{-\gamma' t}\big)\sin Kx_j(0)\Big] \qquad (A.10)$$

$$\delta x_j = -\frac{2e}{m}\cdot\frac{R E_K(t)}{a_0^4}\Big[\big(b_0^2\cos\eta_0 t + 2\gamma\eta_0\sin\eta_0 t - b_0^2 e^{-\gamma t} - \gamma a_0^2 t e^{-\gamma t}\big)\cos Kx_j(0) + \big(b_0^2\sin\eta_0 t - 2\gamma\eta_0\cos\eta_0 t + 2\gamma\eta_0 e^{-\gamma t} + \eta_0 a_0^2 x e^{-\gamma t}\big)\sin Kx_j(0)\Big]$$

$$-\frac{2e}{m}\cdot\frac{R F_K(t)}{a_1^4}\Big[\big(b_1^2\cos\eta_0' t + 2\gamma'\eta_0'\sin\eta_0' t - b_1^2 e^{-\gamma' t} - \gamma' a_1^2 t e^{-\gamma' t}\big)\cos Kx_j(0) + \big(b_1^2\sin\eta_0' t - 2\gamma'\eta_0'\cos\eta_0' t + 2\gamma'\eta_0' e^{-\gamma' t} + \eta_0' a_1^2 t e^{-\gamma' t}\big)\sin Kx_j(0)\Big] \qquad (A.11)$$

where $a_0^2 = \gamma^2 + \eta_0^2$, $a_1^2 = \gamma'^2 + \eta_0'^2$, $b_0^2 = \gamma^2 - \eta_0^2$ and $b_1^2 = \gamma'^2 - \eta_0'^2$. Substituting these values into the right hand side of eqs.(A.1) and (A.2) which are expanded up tc the third order product of δX_j and δV_j, assuming that the initial positions $X_j(0)$ are uniformly distributed and using

$$\frac{1}{N}\sum_j \sin^2 Kx_j(0) = \frac{1}{N}\sum_j \cos^2 Kx_j(0) = \frac{1}{2}\ , \quad \frac{1}{N}\sum_j \sin Kx_j(0)\cdot\cos Kx_j(0) = 0, \qquad (A.12)$$

we find the set of equations (10) and (11).

Referneces

1. E.A.Kornilov, Ya.B.Fainberg, L.I.Bolotin, and O.F.Kovpik, Soviet Phys.-JETP Lett. 3,229(1966).
2. T.Obiki, R.Itatani, and Y.Otani, Phys.Rev.Lett. 20,184(1968).
3. B.E.Keen and W.H.W.Fletcher, Phys.Rev.Lett. 23,760(1969);24,130(1970).
4. Y.Nakamura, J.Phys.Soc.Jpn. 28,1315(1970);31,273(1971).
5. R.Itatani, T.Obiki, and O.Fukumasa, J.Phys.Soc.Jpn. 33,274(1972).
6. P.DeNeef and H.Lashinsky, Phys.Rev.Lett. 31,1039(1973).
7. T.Tsuru, A.Itakura, and S.Kojima, J.Phys.Soc.Jpn. 34,189(1973).
8. O.Fukumasa and R.Itatani, J.Phys.Soc.Jpn. 42,357(1977).
9. O.Fukumasa and R.Itatani, Phys.Lett. 68A,59(1978).
10. O.Fukumasa and R.Itatani, Pro.Inter.Confer.Plasma Phys., Nagoya, Japan, Vol.1 p.234(1980).
11. H.Amemiya, Phys.Lett. 62A,220(1977).
12. H.Amemiya, J.Phys.Soc.Jpn. 47,633(1979).
13. P.Michelsen, H.L.Pecseli, J.J.Rasmussen, and R.Schrittwieser, Plasma Phys. 21,61(1979).
14. T.Kato, T.Okasaki, and T.Ohsawa, J.Phys.Soc.Jpn. 46,277(1979).
15. M.Guillemot, J.Olivain, F.Perceval, and J.Scharer, Phys.Fluids 14,952(1971).
16. A.Itakura, J.Phys.Soc.Jpn. 41,305(1976).
17. M.V.Nezlin, G.I.Sapozhnikov, and A.M.Solntsev, Soviet Phys.-JETP 23,232(1966).
18. R.L.Foek and M.A.Pollack, Phys.Rev. 139,A1408(1965).
19. T.M.O'Neil, J.H.Winfrey, and J.H.Malmberg, Phys.Fluids 14,1204(1971).

20. I.N.Onishchenko, A.R.Linetskii, N.G.Matsiborko, V.D.Shapiro, and V.I.Shevchenko, Soviet Phys.-JETP Lett. 12,281(1970).
21. W.E.Lamb, Phys.Rev. 134,A1429(1964).
22. J.E.Walsh and J.S.Hagelin, Phys.Fluids 19,339(1976).
23. A.E.M.Janssen and J.J.Rasmussen, Risφ Report, Risφ-I-14(1979).
24. H.Böhmer, J.Chang, and M.Raether, Phys.Fluids 14,150(1971).
25. O.Fukumasa, H.Abe, and R.Itatani, Phys.Rev.Lett. 40,393(1978).

Figure captions

Fig.1. Schematic diagram of the beam-plasma system and the experimental set-up.

Fig.2. Current-voltage characteristics of the plane probe. The voltage of G_1 is a parameter. The probe is 3 cm from the energy analyzer and its plane is set toward the analyzer so as to collect the reflected beams. Experimental parameters are as follows: L = 17 cm, V_B = 58 V, I_B = 1.77 mA, V_G = -30 V, and p $\cong 1 \times 10^{-5}$Torr.

Fig.3. Relationship between the beam distribution function and the wave intensity. Gas pressure is a parameter. Distribution functions are measured by using the analyzer and waves are picked up by the coaxial probe. Probe position X_1 is 6 cm from A. n is the mode number. Throughout these measurements, V_B is almost kept 45 eV which is indicated by arrows. Parameters: L = 12 cm, V_G = -10 V, and I_B = (4.2-4.7) mA.

Fig.4. Relationship between the beam distribution functions and the wave intensities in the presence of the reflected beams. V_G is a parameter. Distribution functions are measured by the plane probe whose position X is 11 cm from A. The plane is set toward the gun. Waves are picked up by the coaxial probe. Parameters: L = 17 cm, V_B = 62 V, $I_B \simeq$ 3 mA, and p = 3×10^{-4}Torr.

Fig.5. Characteristics of spontaneously excited electron waves.
(a) Frequency shift of the wave and its mode jump. Plasma length

which is changed by moving the energy analyzer, is a parameter. The probe to pick up oscillation signals is kept 7 cm from A. (b) Relationship between wave frequency and the reciprocal of L, i.e. dispersion relation. Parameters: V_B = 38 V, I_B = 4.5 mA, V_G = -10 V and p = 1.8×10^{-4}Torr.

Fig.6. Two examples of wave suppression. (a) Electron wave E_1 with frequency f_1 is excited spontaneously. f_m is set to be in the vicinity of f_1. Parameters: L = 15 cm, V_B = 37 V, I_B = 3.6 mA, V_G = -10 V and p = 1.1×10^{-4}Torr. (b) Electron wave E_2 with f_2(34MHz) is excited. In this case, f_m is set to be in the vicinity of f_3, which is the frequency of the mode neighboring with E_2. Parameters: L = 11 cm, V_B = 40 V, I_B = 4.6 mA, V_G = -10 V and p = 1.8×10^{-4}Torr.

Fig.7. (a) Critical modulation voltage V_c and the resulting amplitude ϕ_c of the excited wave as a function of modulation frequency f_m. Electron wave E_4 with f_4(51MHz) is excited spontaneously. For reference, the amplitude of E_4 without modulation is indicated by the dotted circle. The probe is kept X_1 from A. (b) Three amplitude patterns of the excited waves with different f_m. They are measured by moving the probe along the plasma column. In all cases, E_4 is almost suppressed because values of V_m correspond to those of V_c shown in (a). Parameters: L = 15 cm, V_B = 42 V, I_B = 2.8 mA, V_G = -10 V and p = 1.4×10^{-4}Torr.

Fig.8. Beam distribution functions in the fulfillment of wave suppression. These are measured by using the analyzer. Both f_m and V_c are

parameters. Their values and experimental conditions are the same as in Fig.7.

Fig.9. V_c and ϕ_c as a function of f_m. f_m is set to be in the vicinity of f_3 which is the frequency of the mode neighboring with E_2. Parameters: L = 11 cm, V_B = 35 V, I_B = 4.5 mA, V_G = -10 V and p = 1.8×10^{-4}Torr.

Fig.10. Amplitude patterns of the electron wave E_2 in (a) and the excited wave E_m in (b) for various modulation voltages. In this case, $V_c \cong 2.1\ V_{p-p}$. Parameters: L = 11 cm, V_B = 38 V, I_B = 4.6 mA, V_G = -10 V and p = 1.7×10^{-4}Torr.

Fig.11. Deformation of the beam distribution function due to the excited wave E_m, relating to the suppression of E_2(shown in Fig.10). The beam acceleration energy U_B, the phase velocity of the electron wave U_{p2}, and that of the excited wave U_{pm} are indicated. The values of U_{p2} and U_{pm} are estimated from the wave patterns without modulation and that with $V_m = 2.1\ V_{p-p}$, respectively.

Fig.12. (a)Spatial variation of the beam distribution function in the presence of the excited wave. These traces are obtained by the axially movable plane probe. As the amplitude of E_2 with f_2(37MHz) is fairly small, suppression occurs with a weak modulation, i.e. $V_m = 0.5\ V_{p-p}$. (b)Beam energy at the peak of the beam distribution function and the amplitude of E_m versus axial position, corresponding to the results shown in (a). U_B is the beam acceleration energy.

U_{pm} is the phase velocity of E_m and is estimated from the wave pattern. Parameters: L = 11 cm, V_B = 42 V, I_B = 5.1 mA, V_G = -10 V and p = 1.7×10^{-4}Torr.

Fig.13. Deformation of beam distribution functions obtained at three different points, relating to the suppression of E_3 with f_3(45MHz). Distribution functions shown in (a) are obtained by using the analyzer, and those shown in (b) and (c) are by using the plane probe. Parameters: L = 12 cm, V_B = 41 V, I_B = 4 mA, V_G = -10 V and p = 2.2×10^{-4}Torr.

Fig.14. Typical examples of wave suppression in the presence of the reflected beams. f_m is a parameter. The electron wave E_4 with f_4(38.5MHz) is excited spontaneously. Waves are picked up by the coaxial probe which is 9 cm from A. The spectrum of E_m is indicated by the arrows. Parameters: L = 17 cm, V_B = 62 V, I_B = 2.95 mA, V_G = -37 V and p = 3×10^{-4}Torr.

Fig.15. V_c and ϕ_c as a function of f_m. The amplitude of E_4 without modulation is indicated by the dotted circle. These wave amplitudes are obtained by the probe which is 9 cm from A. Parameters: L = 17 cm, V_B = 58 V, I_B = 2.5 mA, V_G = -38 V, p = 3.3×10^{-4}Torr, f_4 = 38.2 MHz and Δf = 0.4 MHz.

Fig.16. Beam distribution functions corresponding to the wave suppression. These are measured by the plane probe which is 11 cm from A. Bottom trace is the distribution without modulation. Parameters: L = 17 cm, V_B = 57 V, I_B = 2.6 mA, V_G = -37 V, p = 3.2×10^{-4}Torr, f_4 = 37.8 MHz and Δf = 0.4 MHz.

Fig.17. Wave amplitude versus modulation voltage in the absence of the reflected beams. The electron wave E_3 with f_3(45MHz) is excited. The probe is 4 cm from A in (a), and 7 cm from A in (b). The amplitude of E_3 is represented by circles and that of E_m by triangles. Parameters: L = 12 cm, V_B = 43 V, I_B = 4 mA, V_G = -10 V and $p \approx 2.2 \times 10^{-4}$Torr.

Fig.18. Wave amplitude versus modulation voltage in the presence of the reflected beams. The electron wave E_5 with f_5(44.2MHz) is excited. The probe is 6 cm from A. f_m is 42.6 MHz in (a), and 43.2 MHz in (b). The amplitude of E_5 and that of E_m are represented by circles and triangles, respectively. Open symbols are measured by increasing V_m, and dotted ones are by decreasing V_m. Parameters: L = 17 cm, V_B = 53.5 V, I_B = 3.4 mA, V_G = -28 V and $p = 3 \times 10^{-4}$Torr.

Fig.19. Evolution of wave energy and beam spread in a modulated beam-plasma system, where reflected beams are absent.

Fig.20. Evolution of wave energy and beam spread in a modulated beam-plasma system, where reflected beams are present.

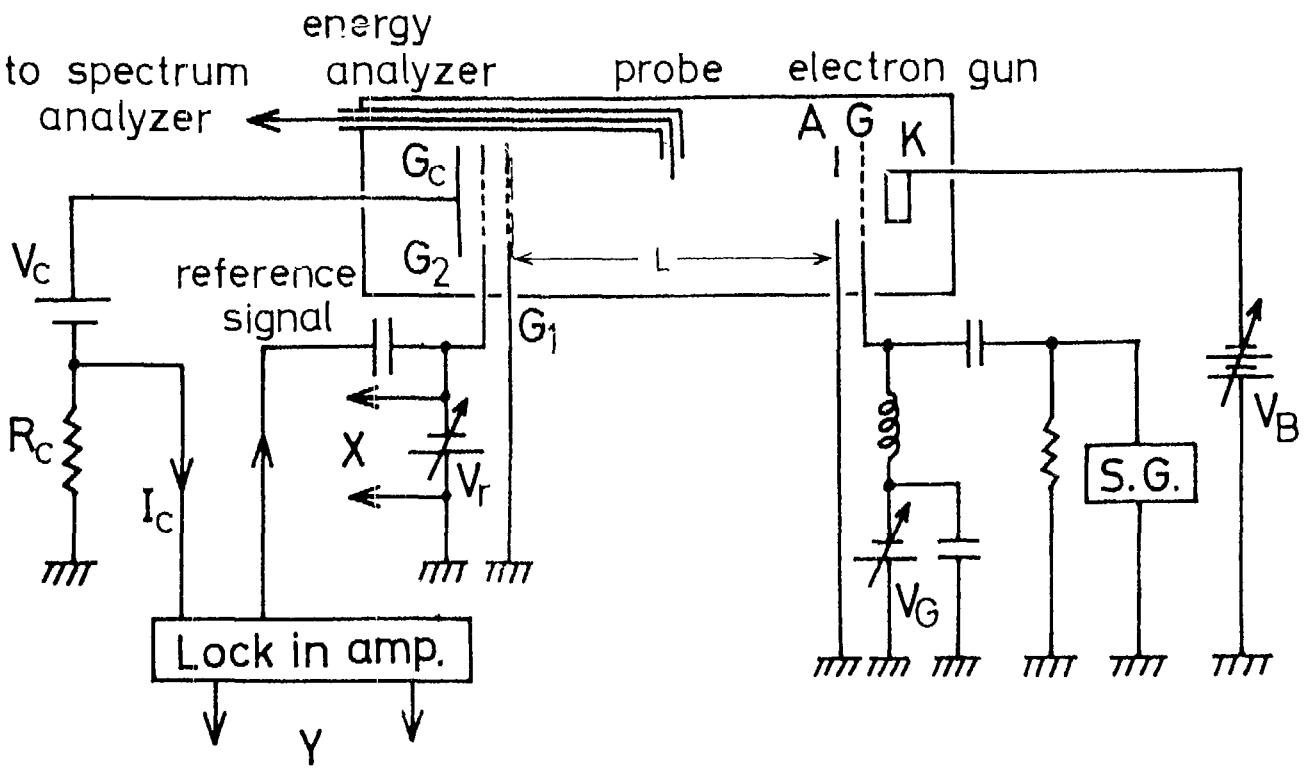
energy
analyzer
to spectrum
analyzer
probe
electron gun
A
G
K
G_c
G_2
G_1
L
V_c
reference
signal
R_c
I_c
X
V_r
V_G
V_B
S.G.
Lock in amp.
Y

Fig.1

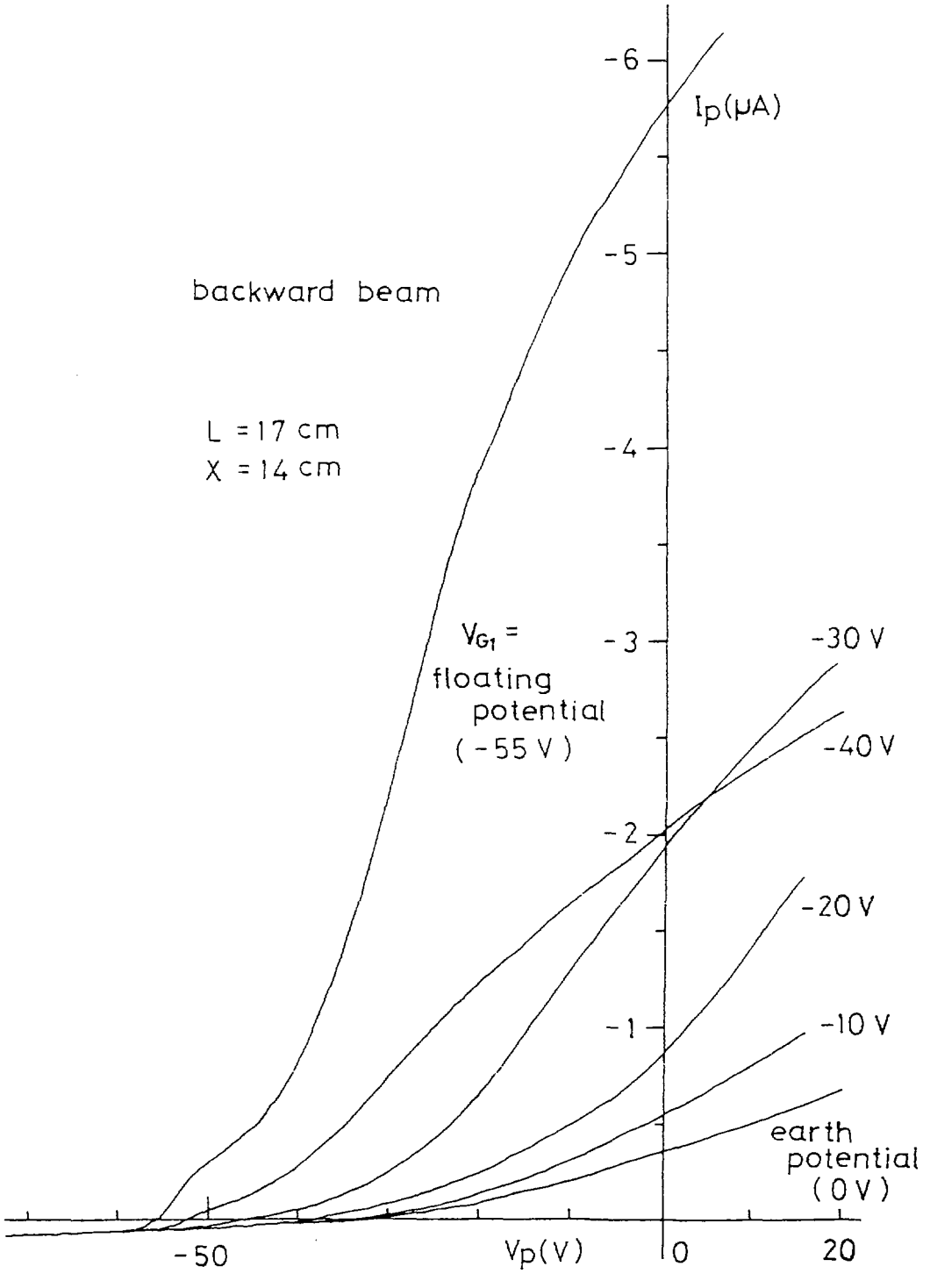
-6
Ip(μA)
backward beam
L = 17 cm
X = 14 cm
-5
-4
V_{G_1} =
floating
potential
(-55 V)
-3
-30 V
-40 V
-2
-20 V
-1
-10 V
earth
potential
(0 V)
-50
Vp(V)
0
20

Fig.2

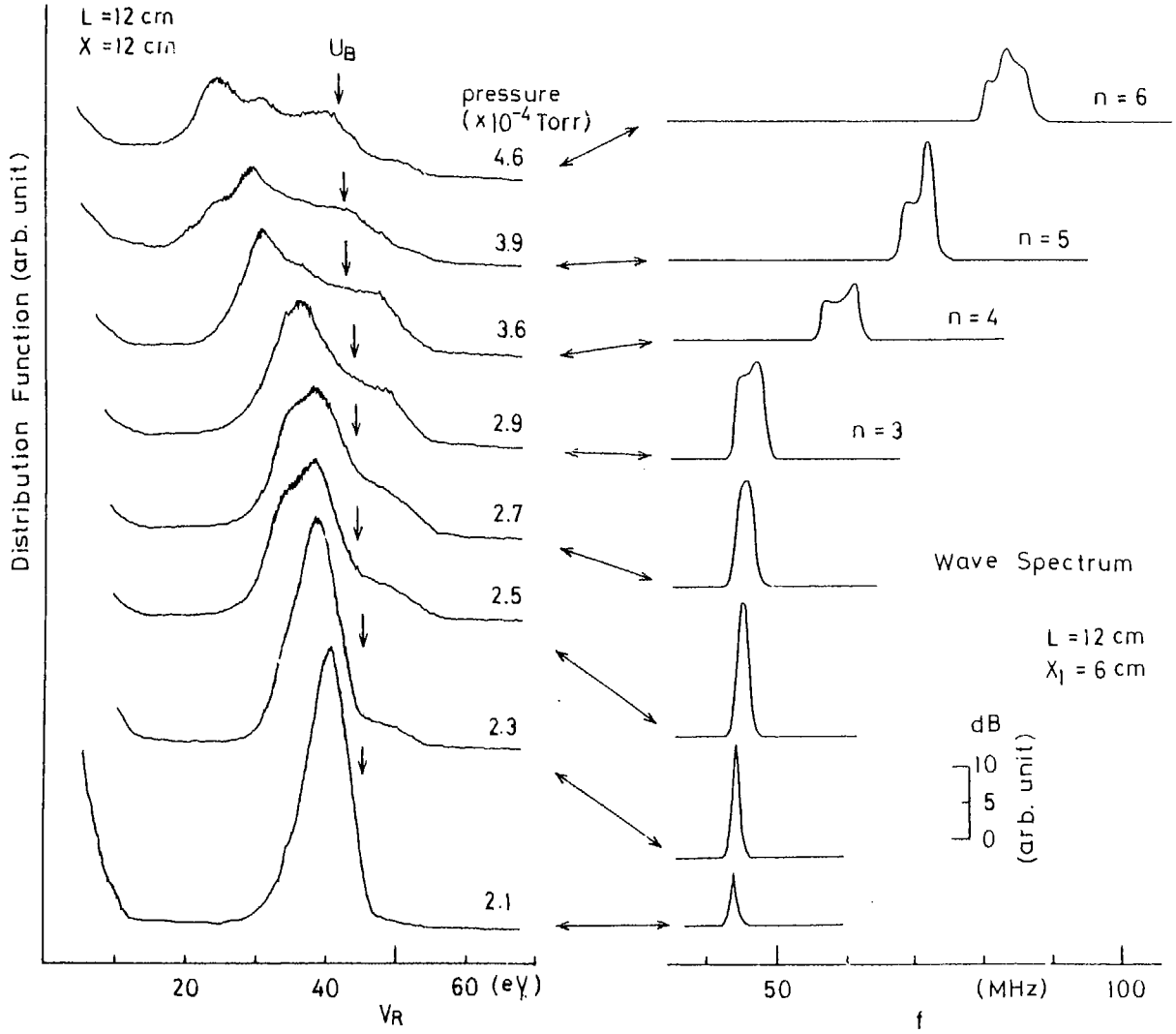
L =12 cm
X =12 cm
U_B
pressure
(x10^{-4} Torr)
4.6
3.9
3.6
2.9
2.7
2.5
2.3
2.1
Distribution Function (arb. unit)
20
40
60 (eV)
V_R
n = 6
n = 5
n = 4
n = 3
Wave Spectrum
L =12 cm
X_1 = 6 cm
dB
10
5
0
(arb. unit)
50
(MHz)
100
f

Fig.3

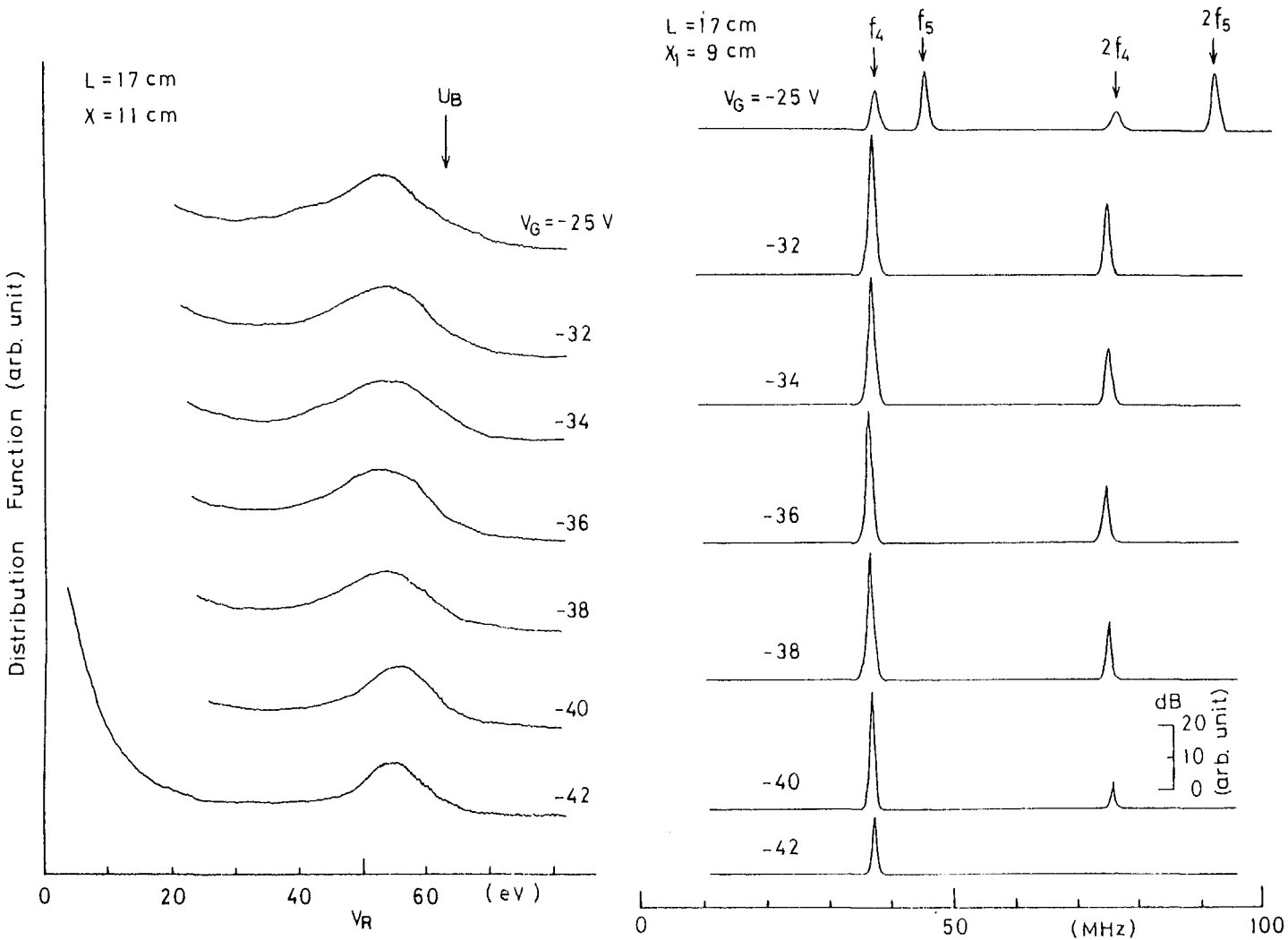
L = 17 cm
X = 11 cm
U_B
V_G = -25 V
-32
-34
-36
-38
-40
-42
Distribution Function (arb. unit)
0
20
40
60
(eV)
V_R
L = 17 cm
X_1 = 9 cm
f_4
f_5
$2f_4$
$2f_5$
V_G = -25 V
-32
-34
-36
-38
-40
-42
dB
20
10
0
(arb. unit)
0
50
(MHz)
100

Fig.4

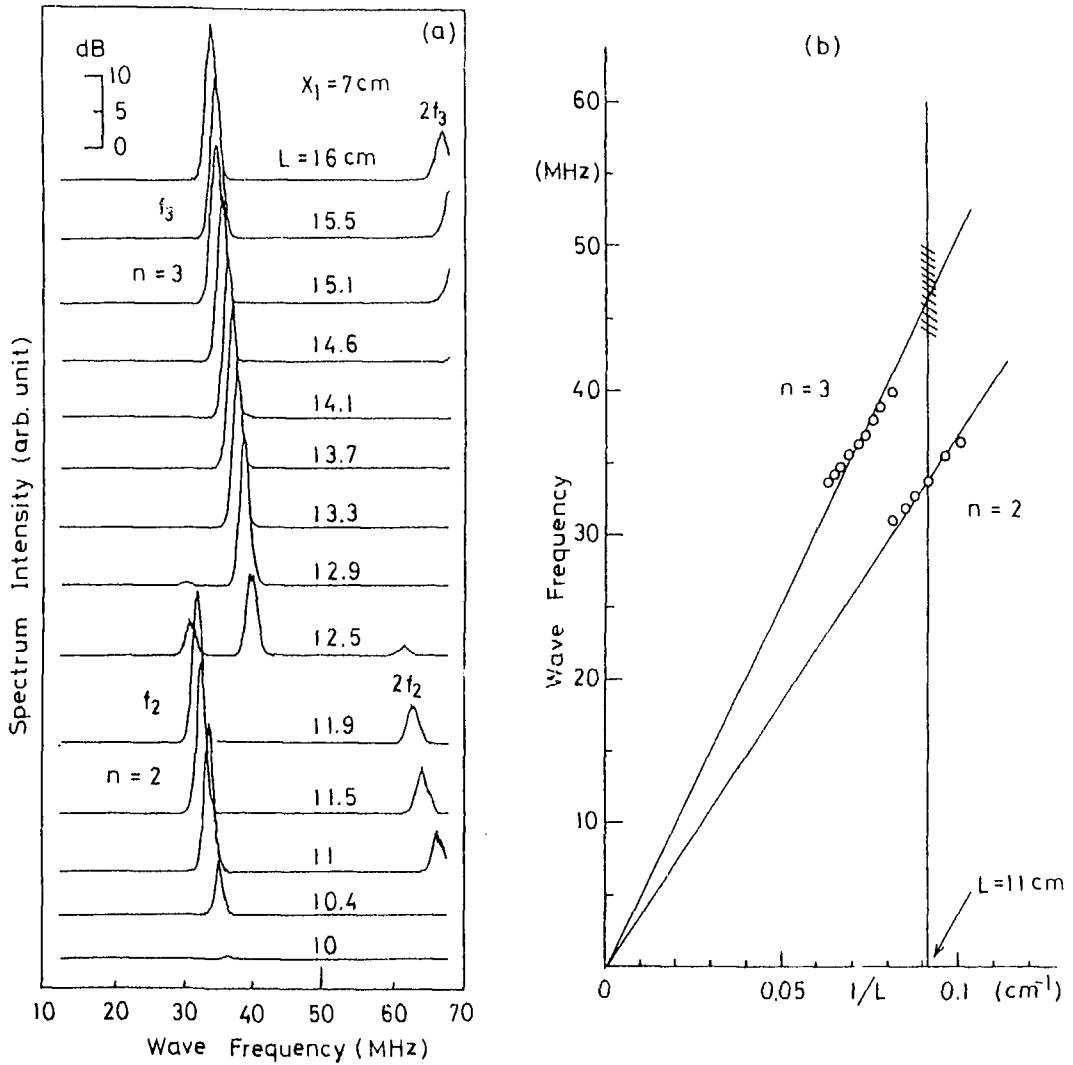
(a)
dB
10
5
0
X_1 = 7 cm
$2f_3$
L = 16 cm
f_3
15.5
n = 3
15.1
14.6
14.1
13.7
13.3
12.9
12.5
$2f_2$
f_2
11.9
n = 2
11.5
11
10.4
10
Spectrum Intensity (arb. unit)
10 20 30 40 50 60 70
Wave Frequency (MHz)
(b)
60
(MHz)
50
40
30
20
10
n = 3
n = 2
L = 11 cm
Wave Frequency
0
0.05
1/L
0.1
(cm^{-1})

Fig.5

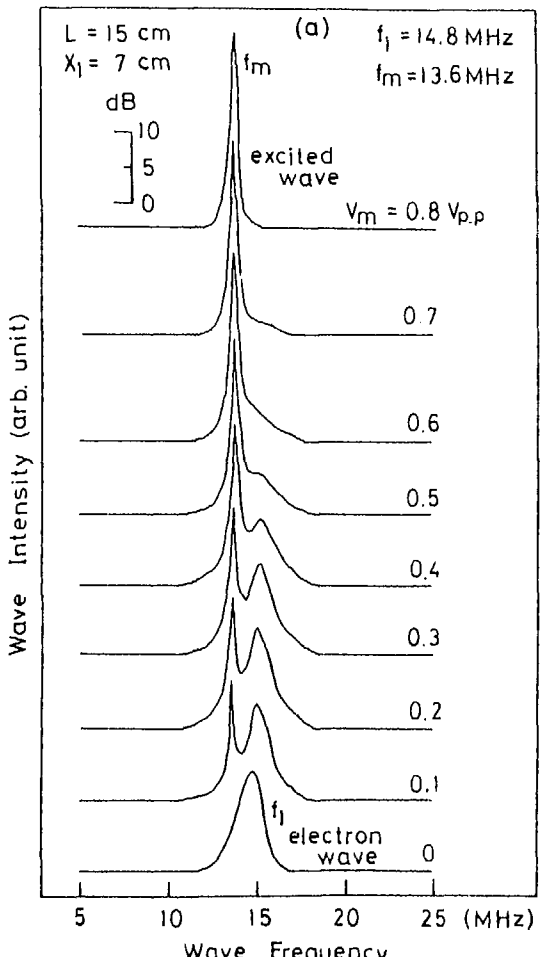
L = 15 cm
X1 = 7 cm
(a)
f1 = 14.8 MHz
fm = 13.6 MHz
fm
dB
10
5
0
excited wave
Vm = 0.8 Vp.p
0.7
0.6
0.5
0.4
0.3
0.2
0.1
f1
electron wave
0
Wave Intensity (arb. unit)
5
10
15
20
25 (MHz)
Wave Frequency

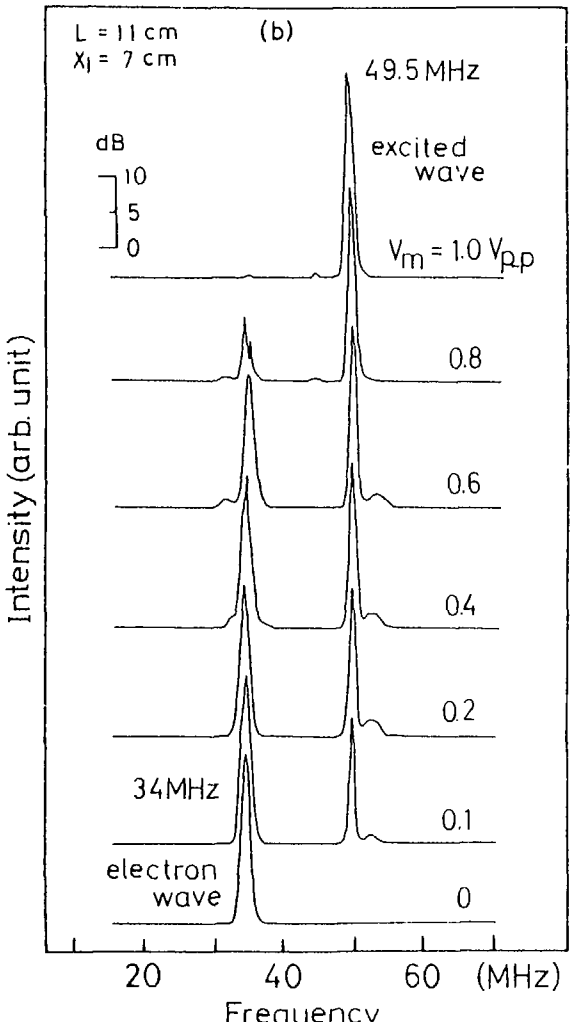
L = 11 cm
X1 = 7 cm
(b)
49.5 MHz
dB
10
5
0
excited wave
Vm = 1.0 Vp.p
0.8
0.6
0.4
0.2
34MHz
0.1
electron wave
0
Intensity (arb. unit)
20
40
60 (MHz)
Frequency

Fig.6

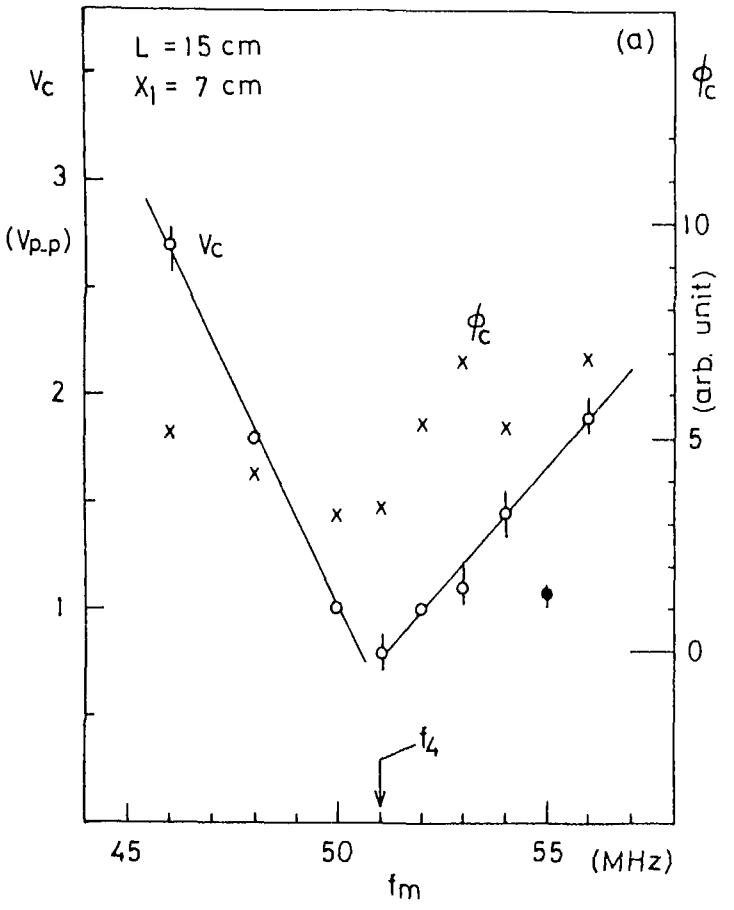
L = 15 cm
X1 = 7 cm
(a)
Vc
(Vp-p)
3
2
1
Vc
φc
10
5
0
(arb. unit)
f4
45
50
55
(MHz)
fm

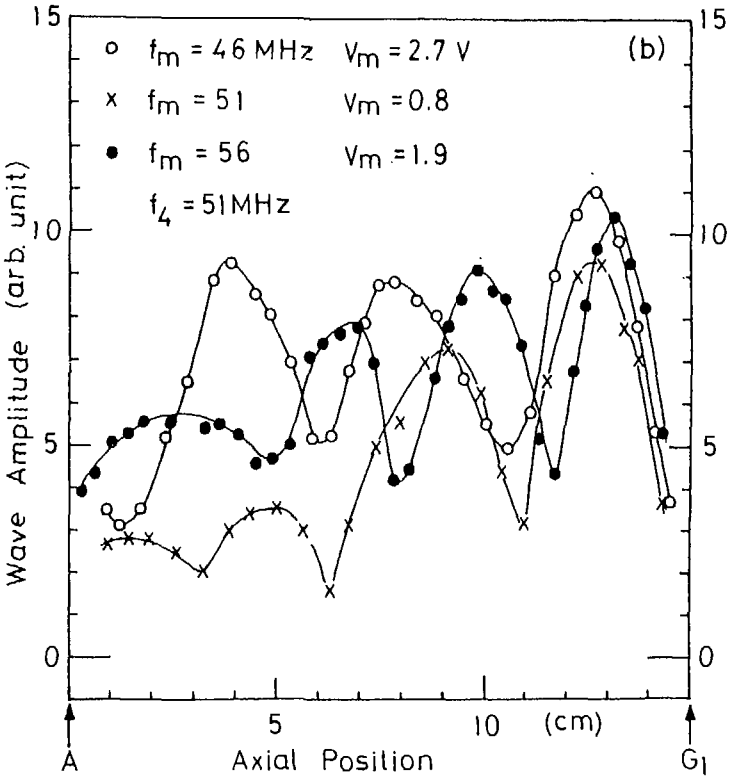
fm = 46 MHz
Vm = 2.7 V
fm = 51
Vm = 0.8
fm = 56
Vm = 1.9
f4 = 51MHz
(b)
15
10
5
0
Wave Amplitude (arb. unit)
5
10
(cm)
A
Axial Position
G1

Fig.7

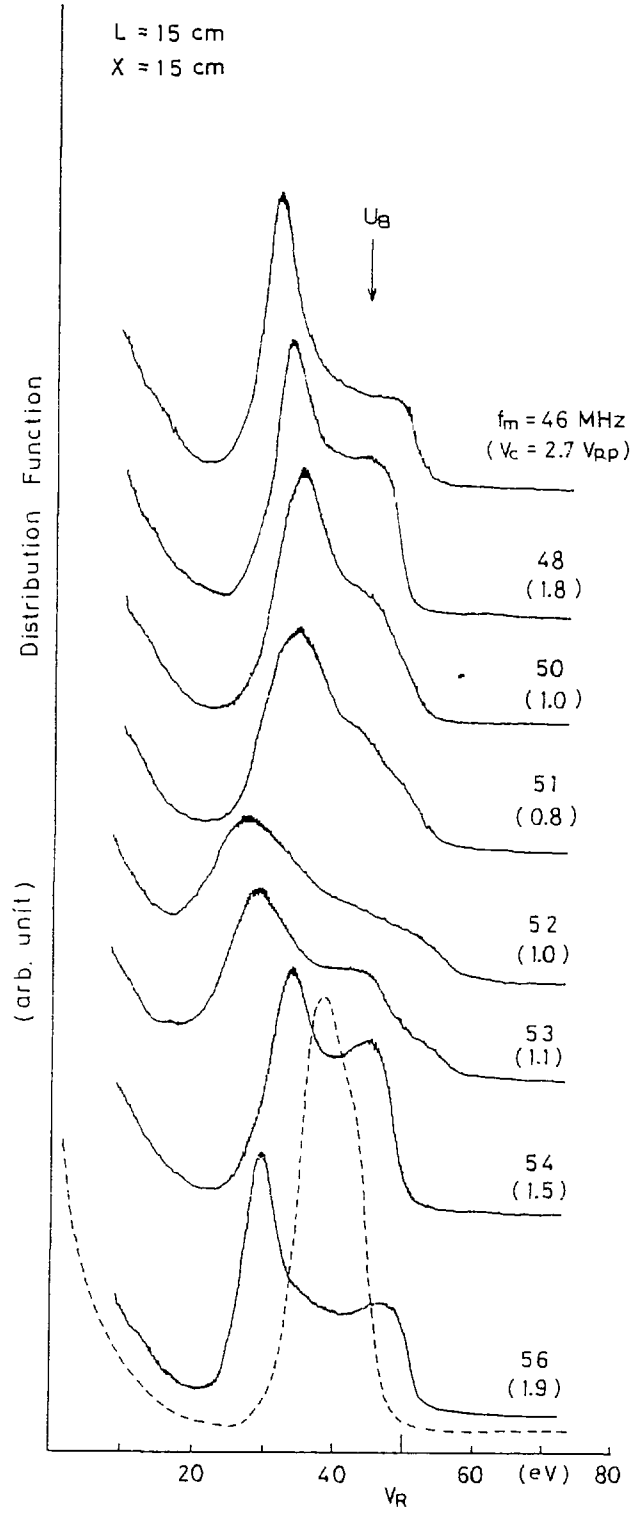
L = 15 cm
X = 15 cm
U_B
f_m = 46 MHz
(V_c = 2.7 V_{pp})
48
(1.8)
50
(1.0)
51
(0.8)
52
(1.0)
53
(1.1)
54
(1.5)
56
(1.9)
Distribution Function
(arb. unit)
20
40
60
(eV)
80
V_R

Fig.8

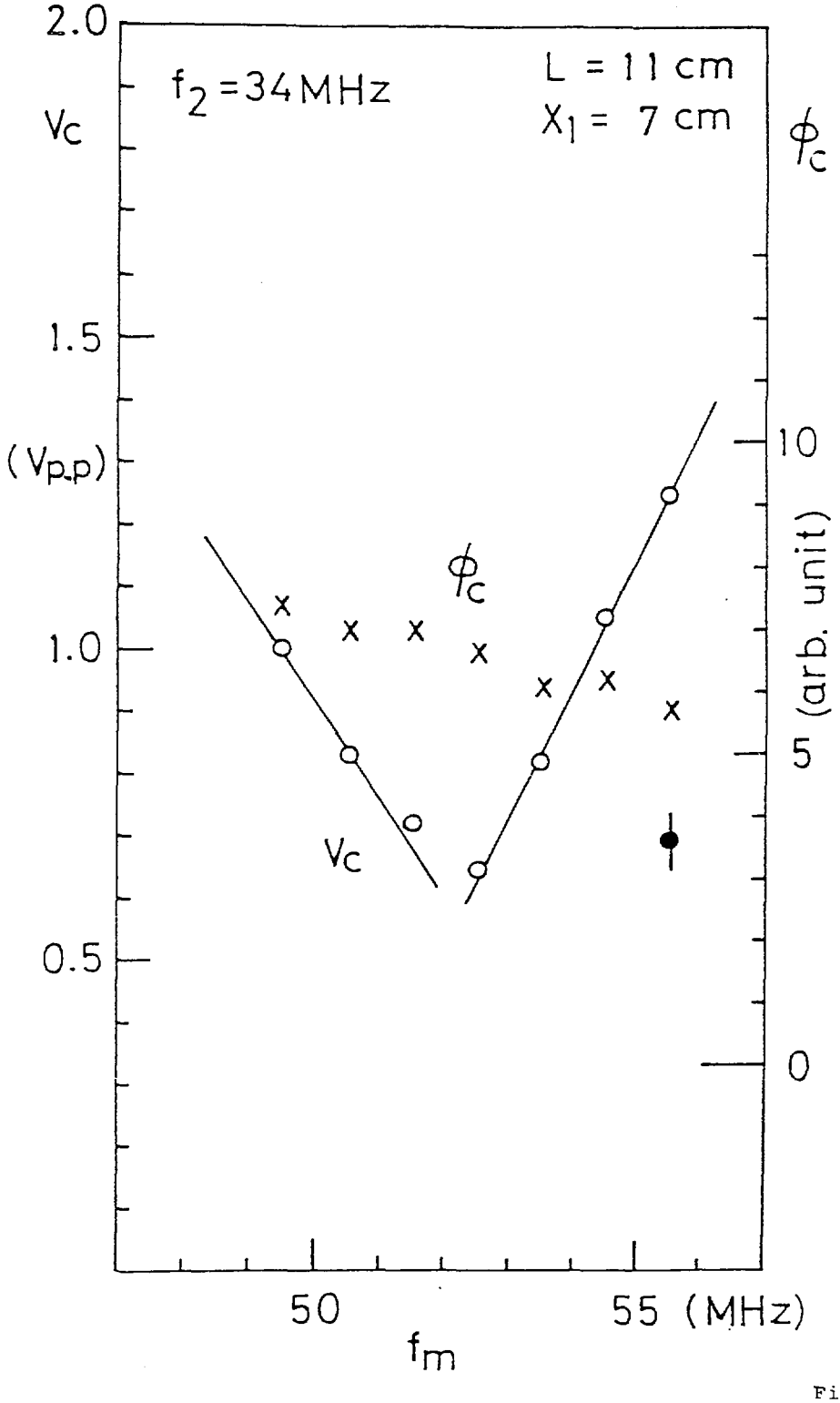
2.0
1.5
1.0
0.5
Vc
(Vp-p)
f2 =34MHz
L = 11 cm
X1 = 7 cm
φc
10
5
0
(arb. unit)
50
55 (MHz)
fm

Fig.9

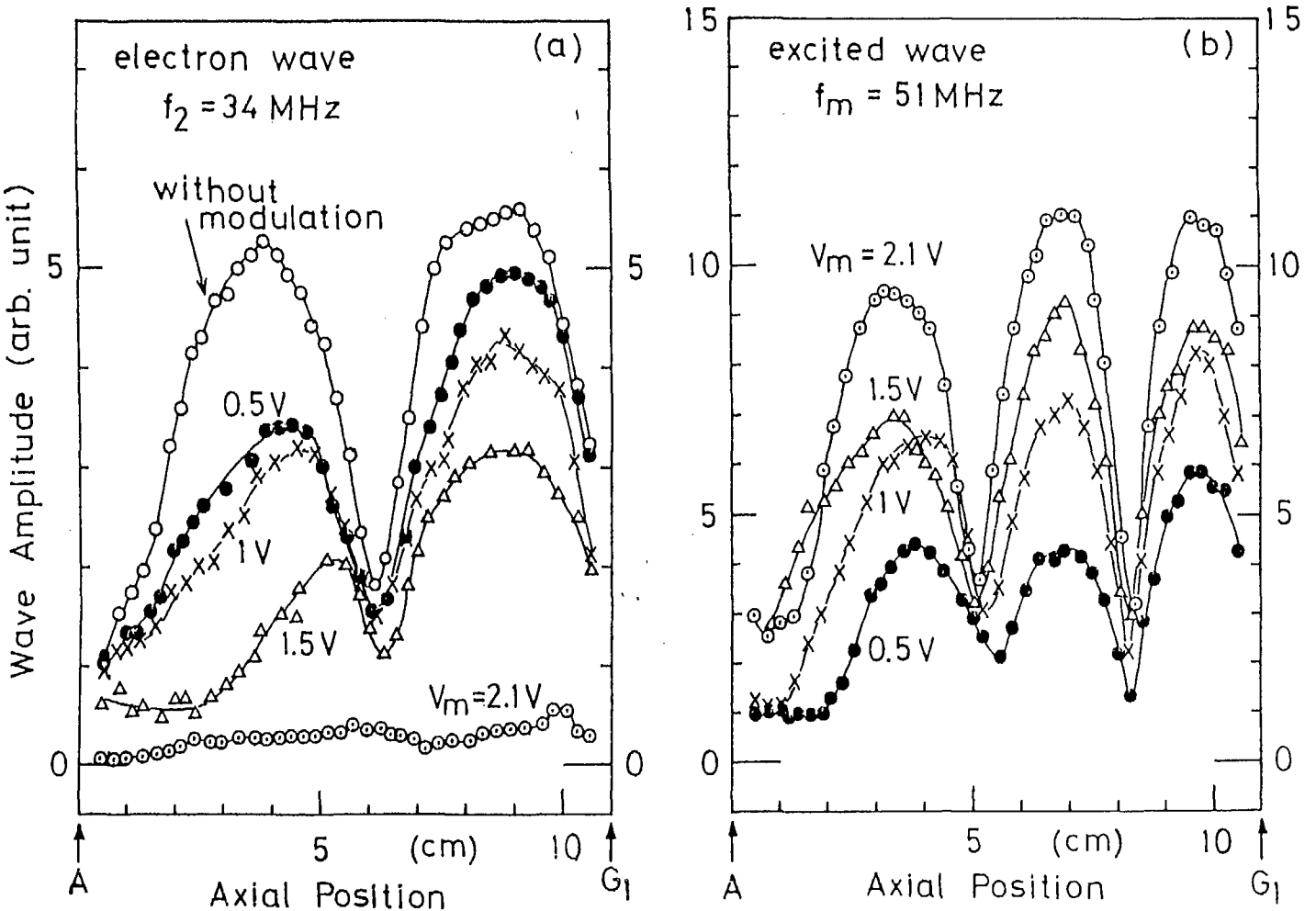
electron wave
(a)
f_2 = 34 MHz
without modulation
0.5V
1V
1.5V
V_m=2.1V
Wave Amplitude (arb. unit)
0
5
A
5
(cm)
10
G_1
Axial Position
excited wave
(b)
f_m = 51MHz
V_m = 2.1 V
1.5V
1V
0.5V
0
5
10
15
A
5
(cm)
10
G_1
Axial Position

Fig.10

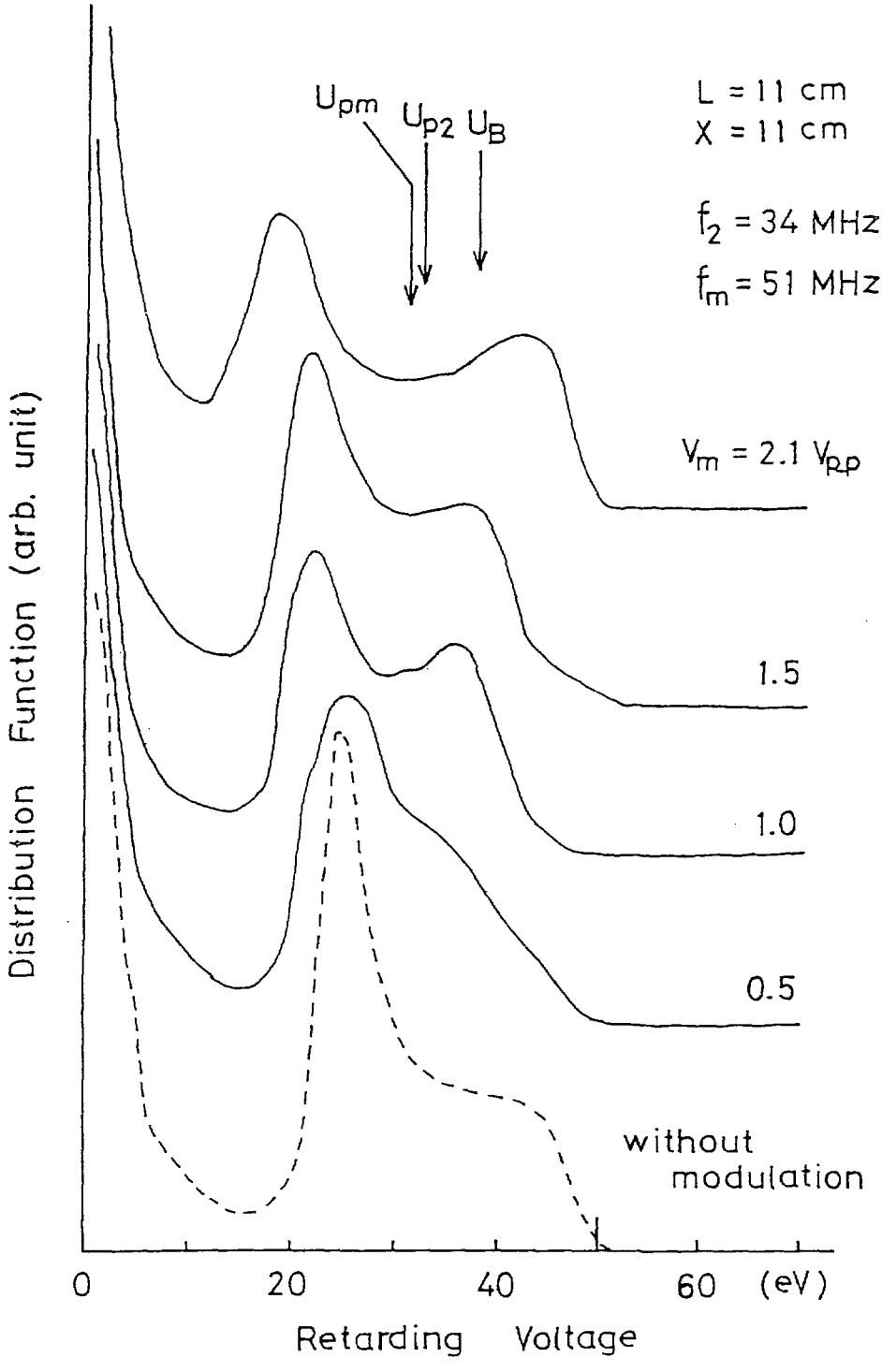
Upm
Up2
UB
L = 11 cm
X = 11 cm
f2 = 34 MHz
fm = 51 MHz
Vm = 2.1 VP-P
1.5
1.0
0.5
without modulation
Distribution Function (arb. unit)
0
20
40
60
(eV)
Retarding Voltage

Fig.11

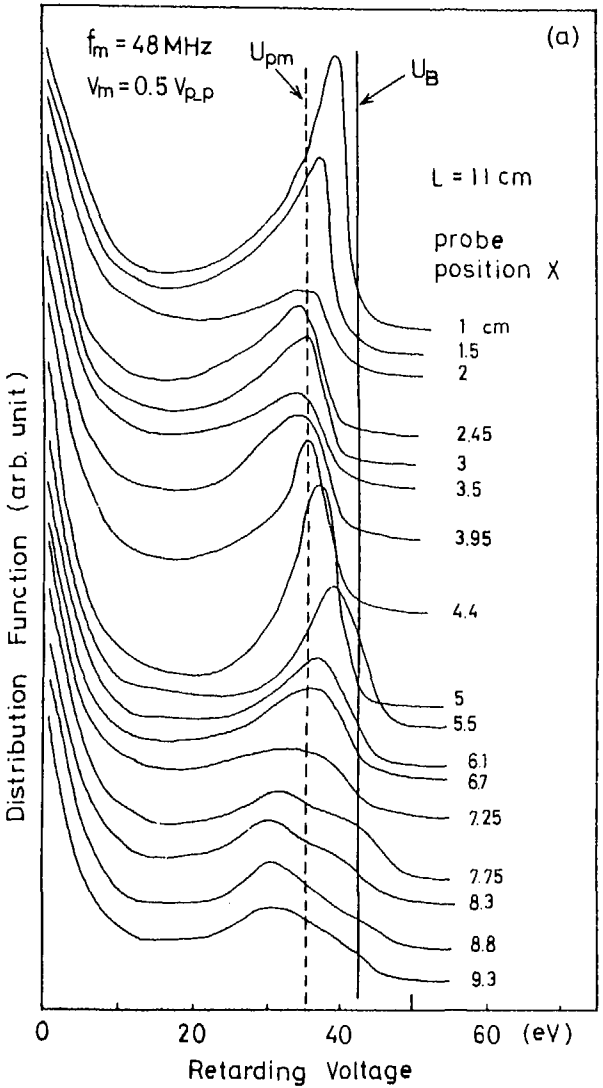
(a)
f_m = 48 MHz
V_m = 0.5 V_{p-p}
U_{pm}
U_B
L = 11 cm
probe position X
1 cm
1.5
2
2.45
3
3.5
3.95
4.4
5
5.5
6.1
6.7
7.25
7.75
8.3
8.8
9.3
Distribution Function (arb. unit)
0
20
40
60 (eV)
Retarding Voltage

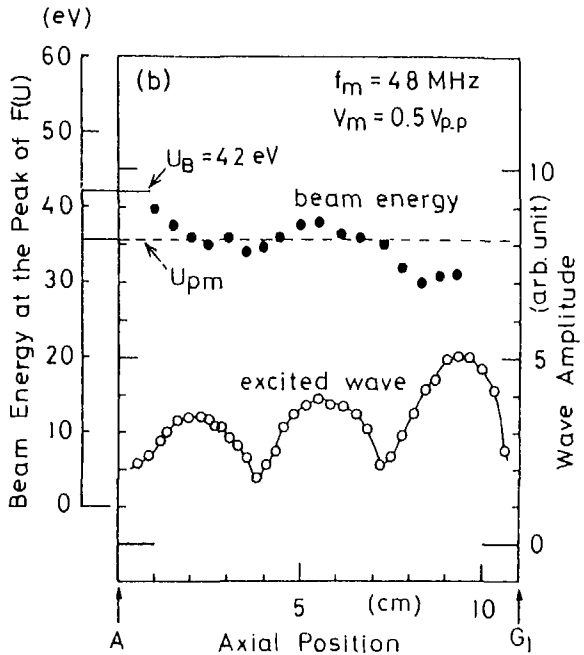
(eV)
(b)
f_m = 48 MHz
V_m = 0.5 V_{p-p}
U_B = 42 eV
beam energy
U_{pm}
excited wave
Beam Energy at the Peak of F(U)
60
50
40
30
20
10
0
10
5
0
(arb. unit)
Wave Amplitude
A
5
(cm)
10
Axial Position
G_1

Fig.12

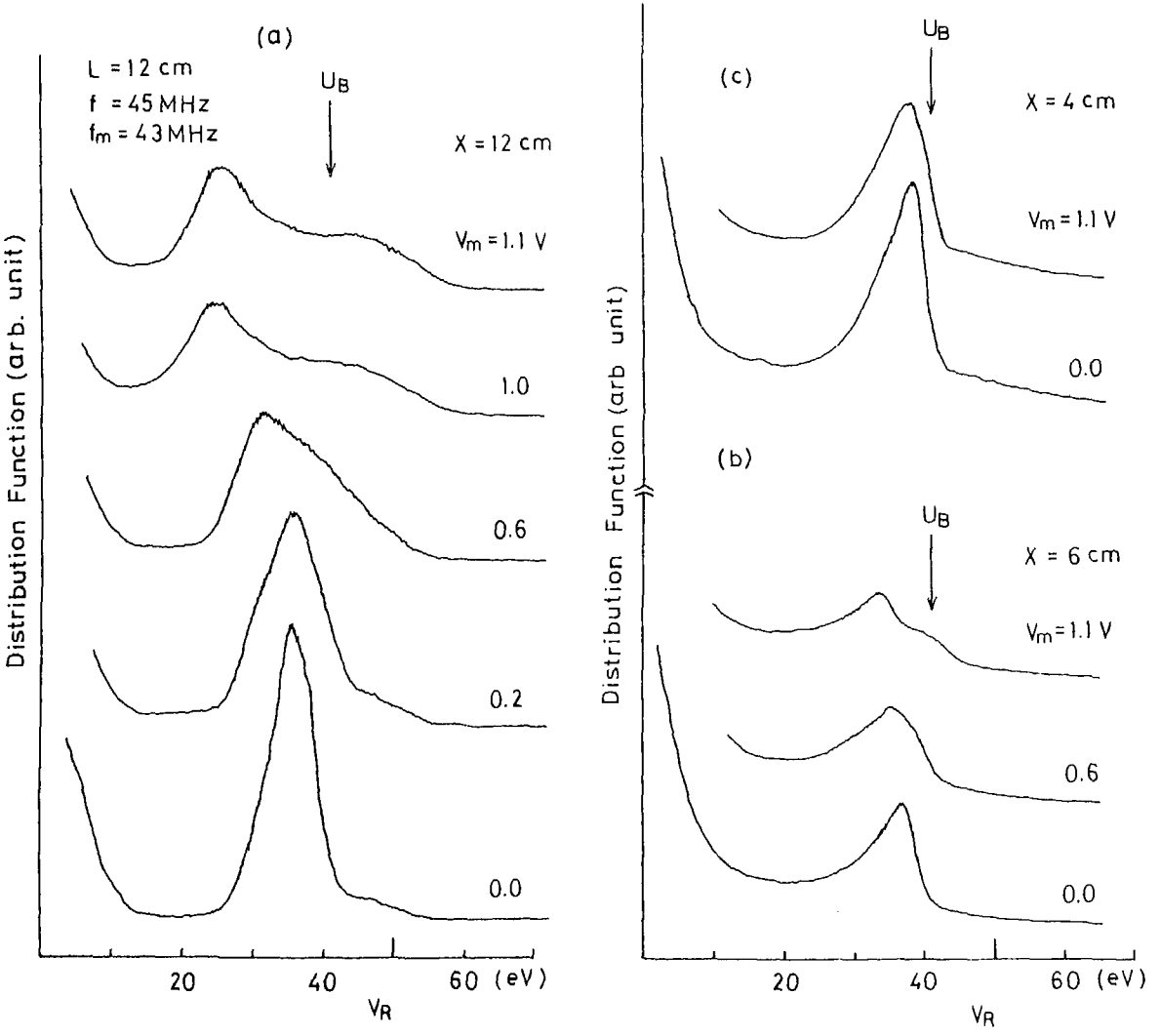
(a)
L = 12 cm
f = 45 MHz
fm = 43 MHz
UB
X = 12 cm
Vm = 1.1 V
1.0
0.6
0.2
0.0
Distribution Function (arb. unit)
20
40
60 (eV)
VR
(c)
UB
X = 4 cm
Vm = 1.1 V
0.0
(b)
UB
X = 6 cm
Vm = 1.1 V
0.6
0.0
Distribution Function (arb unit)
20
40
60 (eV)
VR

Fig.13

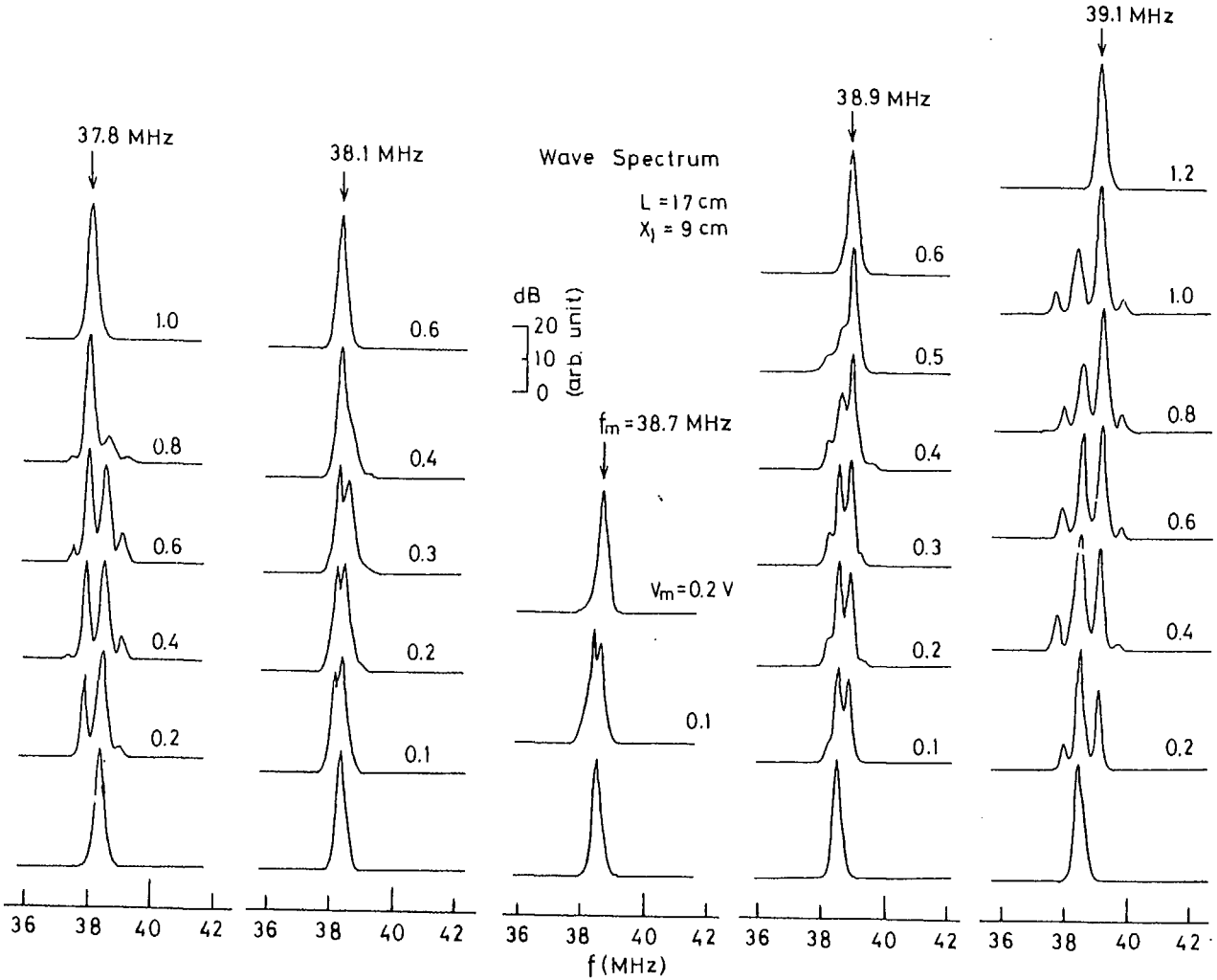
37.8 MHz
38.1 MHz
Wave Spectrum
L = 17 cm
X_J = 9 cm
38.9 MHz
39.1 MHz
dB
20
10
0
(arb. unit)
f_m = 38.7 MHz
V_m = 0.2 V
1.0
0.8
0.6
0.4
0.2
0.6
0.4
0.3
0.2
0.1
0.1
0.6
0.5
0.4
0.3
0.2
0.1
1.2
1.0
0.8
0.6
0.4
0.2
36
38
40
42
f (MHz)

Fig.14

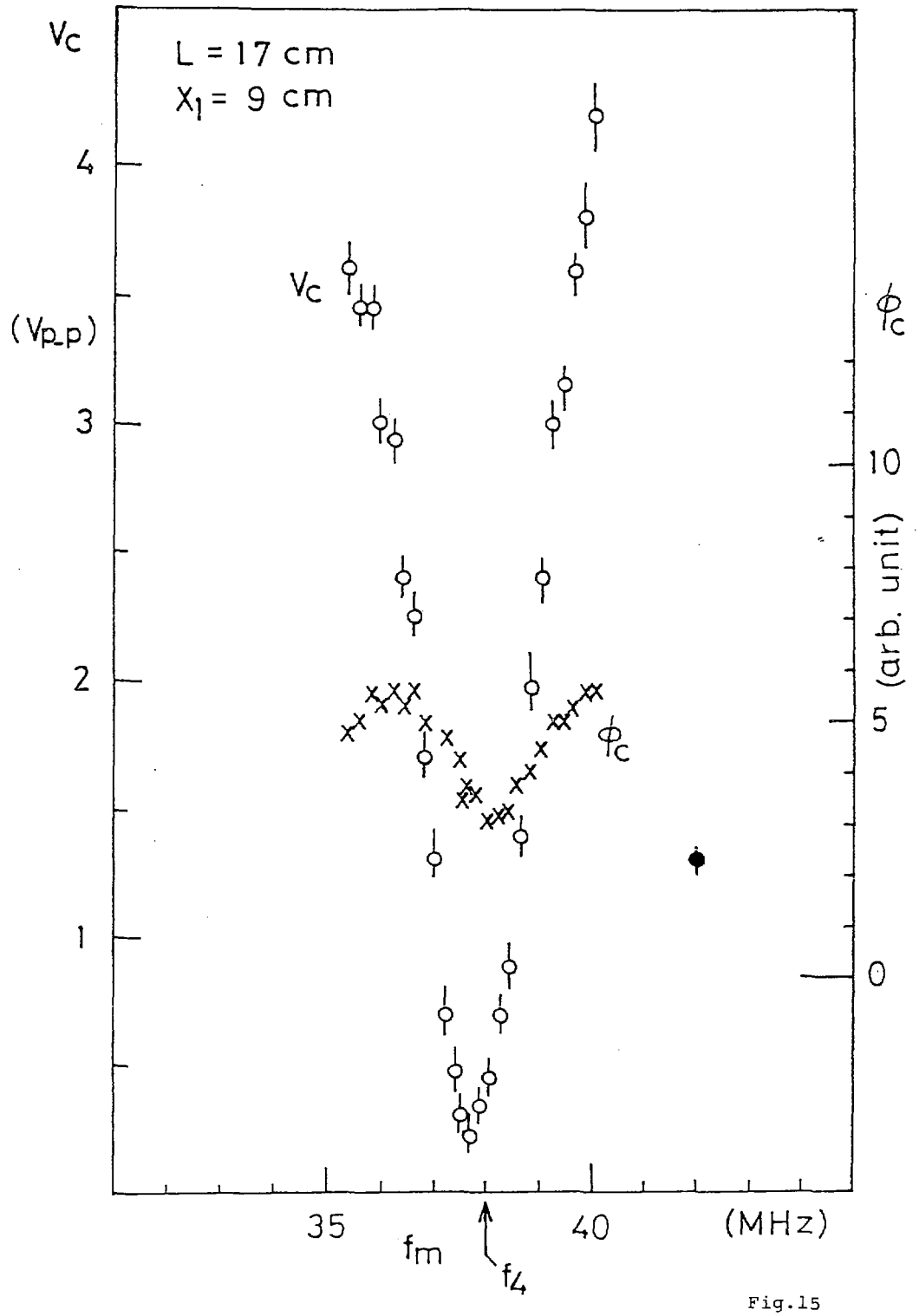

Fig.15

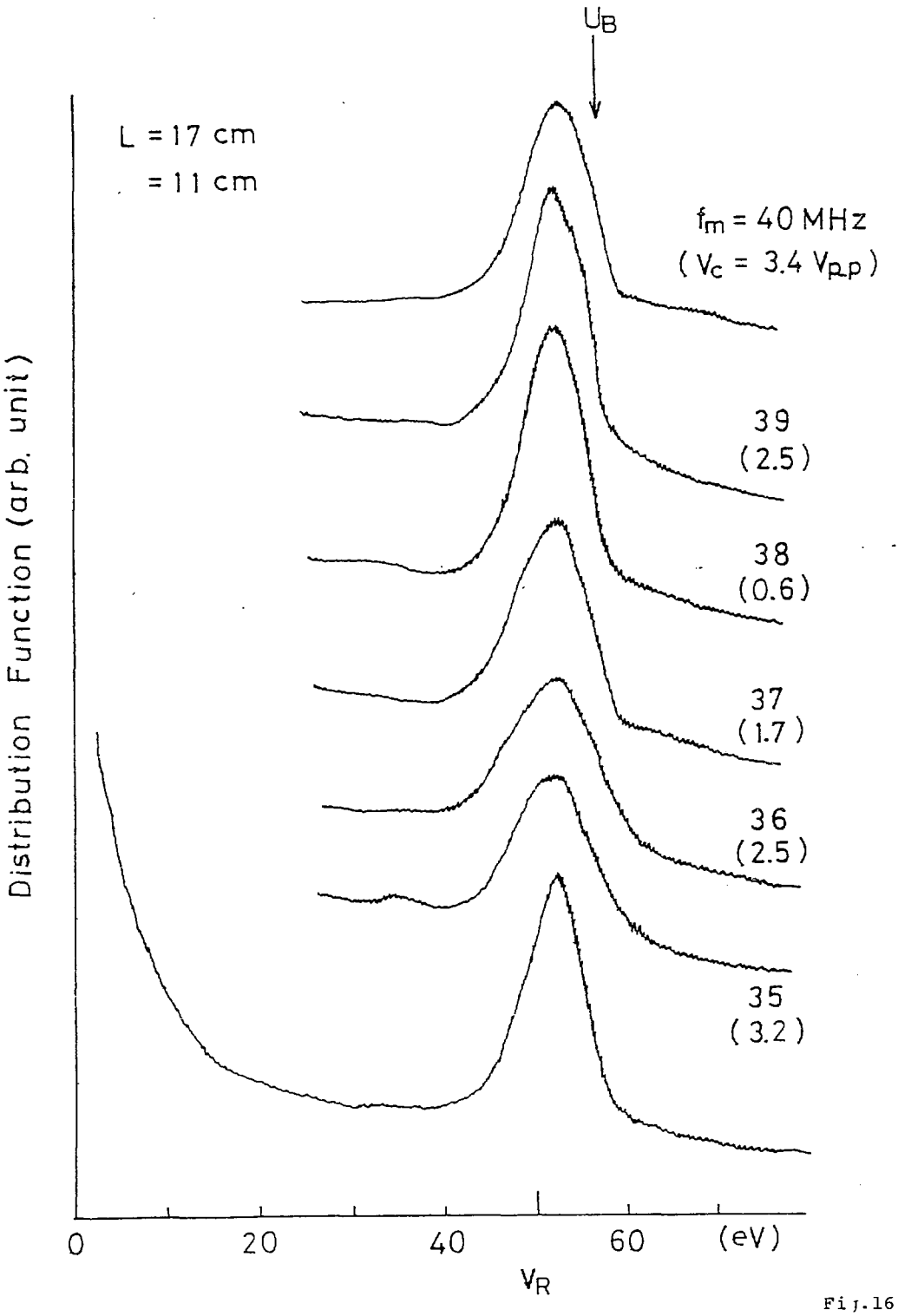
U_B
L = 17 cm
= 11 cm
f_m = 40 MHz
(V_c = 3.4 $V_{p.p}$)
39
(2.5)
38
(0.6)
37
(1.7)
36
(2.5)
35
(3.2)
Distribution Function (arb. unit)
0
20
40
60
(eV)
V_R

Fij.16

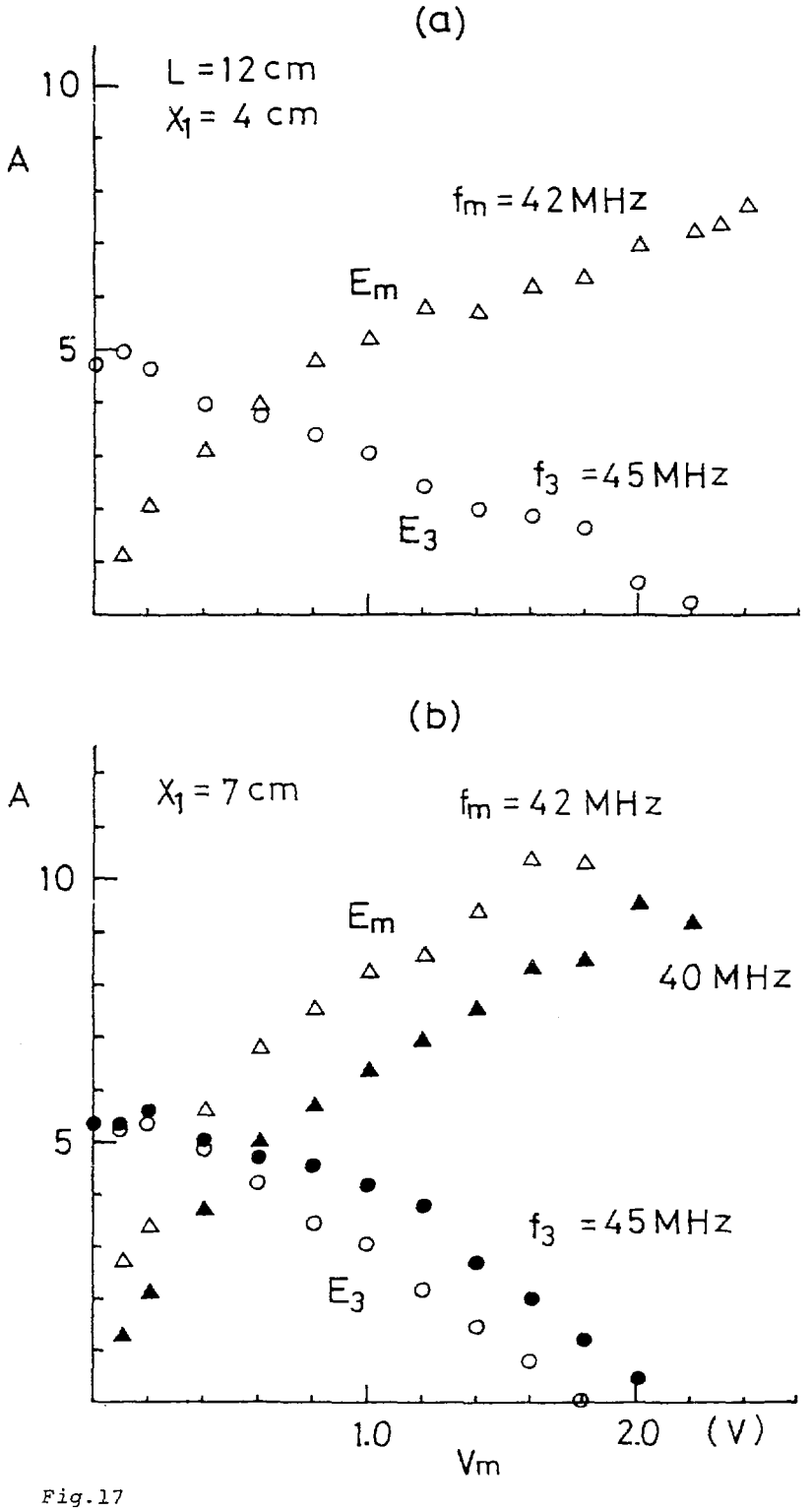
(a)
L = 12 cm
X1 = 4 cm
A
10
5
fm = 42 MHz
Em
f3 = 45 MHz
E3
(b)
X1 = 7 cm
fm = 42 MHz
40 MHz
1.0
2.0
(V)
Vm

Fig.17

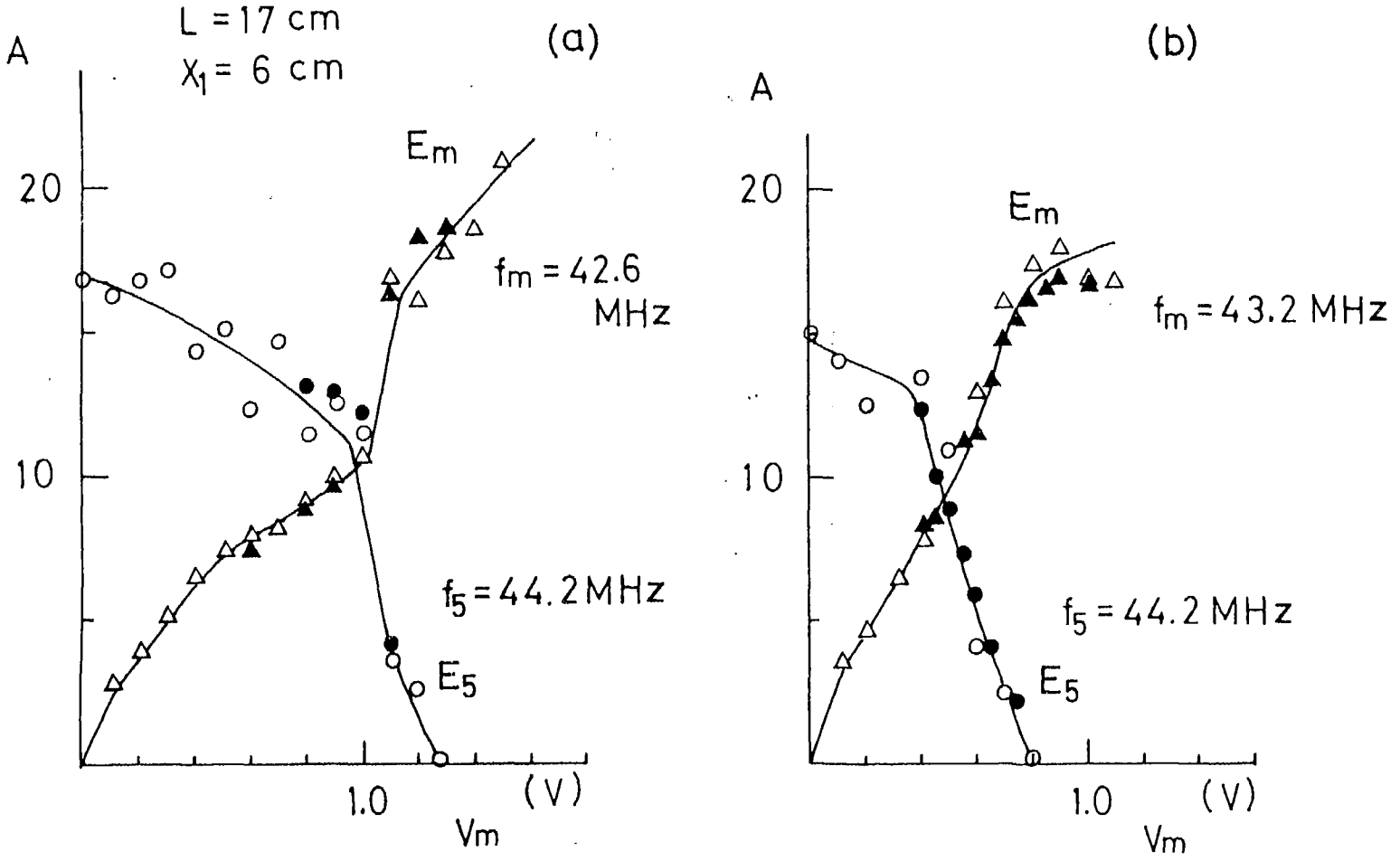
L = 17 cm
X1 = 6 cm
(a)
A
20
10
Em
fm = 42.6 MHz
f5 = 44.2 MHz
E5
1.0
(V)
Vm
(b)
A
20
10
Em
fm = 43.2 MHz
f5 = 44.2 MHz
E5
1.0
(V)
Vm

Fig.18

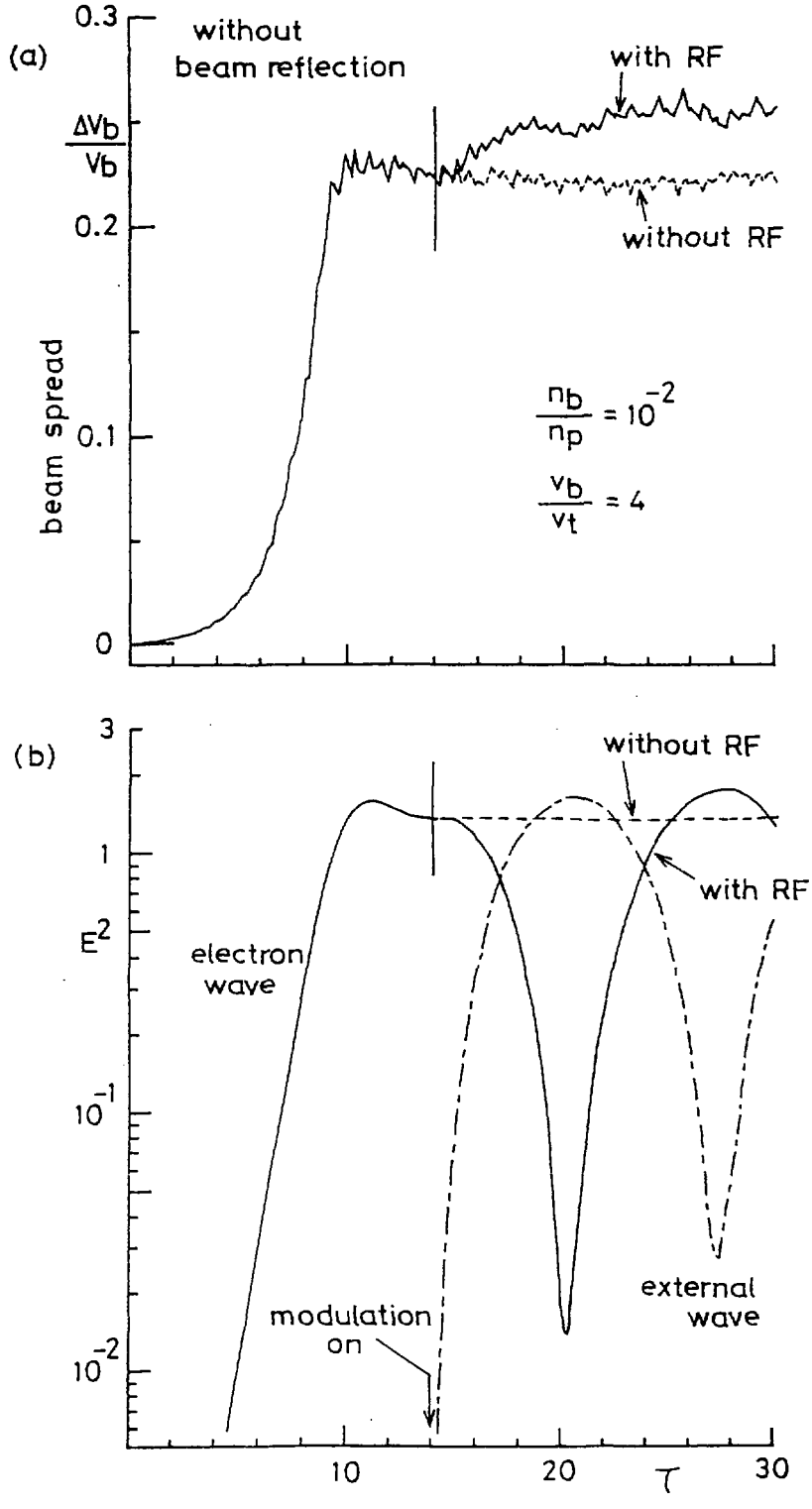
(a)
without
beam reflection
with RF
without RF
ΔVb/Vb
beam spread
0.3
0.2
0.1
0
nb/np = 10^-2
vb/vt = 4
(b)
without RF
with RF
electron
wave
external
wave
modulation
on
E^2
3
1
10^-1
10^-2
10
20
τ
30

Fig.19

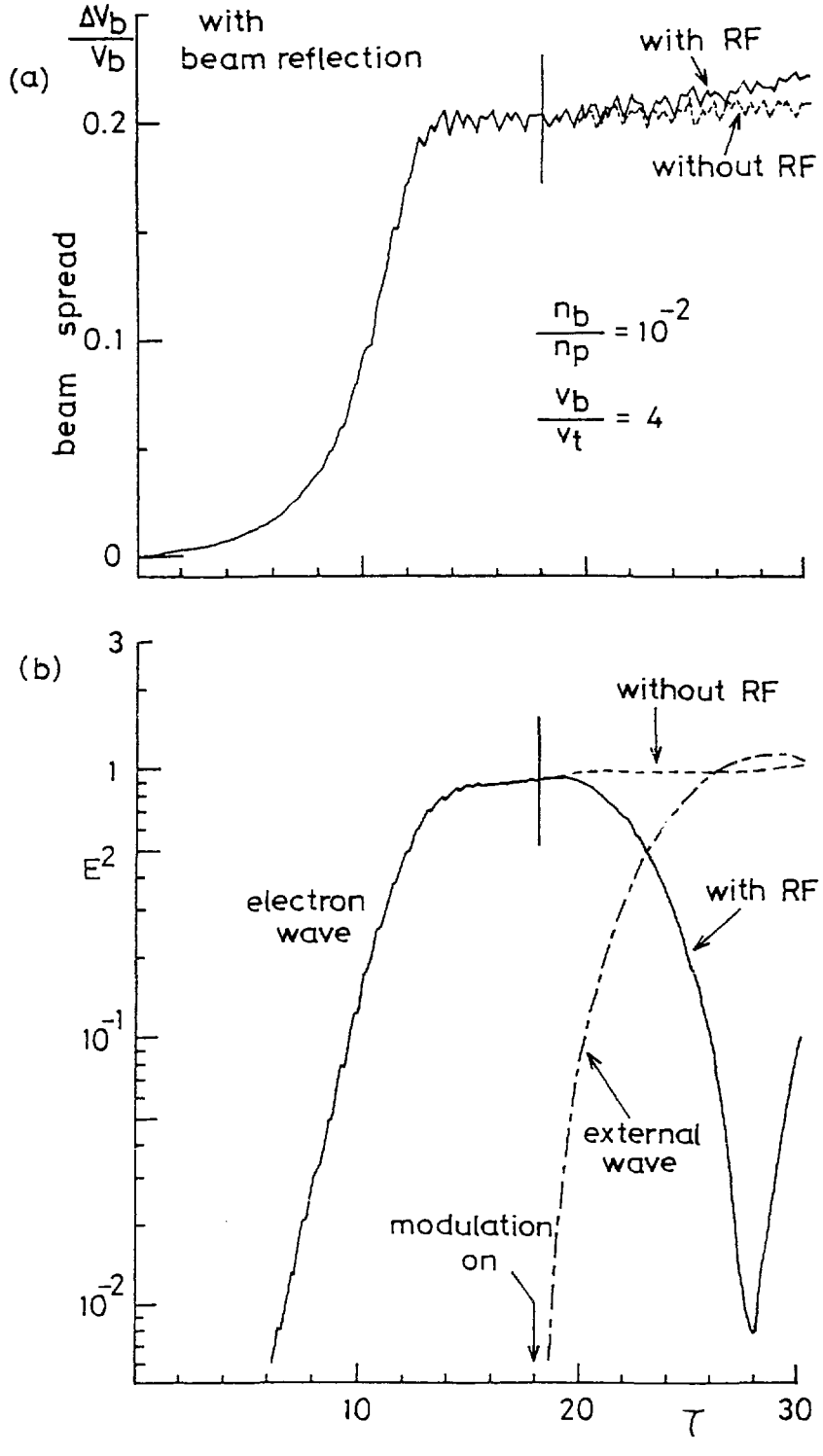
(a)
ΔVb/Vb
with beam reflection
with RF
without RF
0.2
0.1
0
beam spread
nb/np = 10^-2
vb/vt = 4
(b)
3
1
10^-1
10^-2
E^2
without RF
with RF
electron wave
external wave
modulation on
10
20
30
τ

Fig.20